Phase transition and thermodynamic geometry of topological dilaton black holes in gravitating logarithmic nonlinear electrodynamics

A. Sheykhi,[1,2,*] F. Naeimipour,[1] and S. M. Zebarjad[1,†]

[1]*Physics Department and Biruni Observatory, College of Sciences, Shiraz University, Shiraz 71454, Iran*
[2]*Research Institute for Astronomy and Astrophysics of Maragha (RIAAM), P.O. Box 55134-441 Maragha, Iran*

(Received 24 January 2015; revised manuscript received 20 April 2015; published 18 June 2015)

Considering the Lagrangian of the logarithmic nonlinear electrodynamics in the presence of a scalar dilaton field, we obtain a new class of topological black hole solutions of Einstein-dilaton gravity with two Liouville-type dilaton potentials. Black hole horizons and cosmological horizons, in these spacetimes, can be a two-dimensional positive, zero, or negative constant curvature surface. We find that the behavior of the electric field crucially depends on the dilaton coupling constant α. For small α, the electric field diverges *near the origin*, although its divergency is weaker than the linear Maxwell field. However, with increasing α, the behavior of the electric field, *near the origin*, approaches to that of the Maxwell field. We also study casual structure, asymptotic behavior, and physical properties of the solutions. We find that, depending on the model parameters, the topological dilaton black holes may have one or two horizons, and even in some cases we encounter a naked singularity without horizon. We compute the conserved and thermodynamic quantities of the spacetime and investigate that these quantities satisfy the first law of thermodynamics. We also probe thermal stability in the canonical and grand canonical ensembles and disclose the effects of the dilaton field as well as nonlinear parameter on the thermal stability of the solutions. Finally, we investigate thermodynamical geometry of the obtained solutions by introducing a new metric and studying the phase transition points due to the divergency of the Ricci scalar. We find that the dilaton field affects the phase transition points of the system.

DOI: 10.1103/PhysRevD.91.124057 PACS numbers: 04.70.-s, 04.30.-w

I. INTRODUCTION

Nowadays, it is a general belief that the Einstein theory of gravity can be understood as the low energy limit of superstring theory. Indeed, it has been shown that string theory in the low energy limit leads to the Einstein gravity, coupled nonminimally to a scalar dilaton field [1]. Although one can consistently truncate such models to consider, the presence of the dilaton field cannot be ignored if one considers coupling of the gravity to other gauge fields, and thus the dilaton field is an essential feather of the string theory. The coupling of the dilaton field with another gauge field has profound consequences on the behavior of the solutions. For example, in the presence of one or two Liouville-type potentials, it has been shown that there exist dilaton black holes/branes solutions in which their asymptotic behavior is neither flat nor anti-de Sitter (AdS) [2–14]. There are two motivations for studying nonasymptotically flat or AdS black hole spacetimes. First, these solutions can shed some light on the possible extensions of AdS/Conformal Field theory (CFT) correspondence. Second, such solutions may be used to extend the range of validity of methods and tools originally developed for, and tested in the case of, asymptotically flat or asymptotically AdS black holes.

In this paper, we will study topological dilaton black holes in the presence of nonlinear electrodynamics. The theory of the nonlinear electrodynamics has a long history since the pioneering work of Born and Infeld (BI) in 1934 [15]. By extension the linear Maxwell Lagrangian $L = -F_{\mu\nu}F^{\mu\nu}$ to the nonlinear Lagrangian,

$$L_{\rm BI} = 4\beta^2\left(1 - \sqrt{1 + \frac{F_{\mu\nu}F^{\mu\nu}}{2\beta^2}}\right), \tag{1}$$

the first trying was made to resolve various problems appearing in the classical linear electrodynamics [15]. For example, in Maxwell theory, the self-energy of a pointlike charged particle becomes infinite and the electric field of such a particle diverges at exactly its location. In the above expression β is called the nonlinear parameter with dimension of mass and $F_{\mu\nu}$ is the electromagnetic field tensor. In the limiting case where $\beta \to \infty$, the nonlinear Lagrangian (1) reduces to the linear Maxwell Lagrangian.

In recent years, there has been renewed interest in nonlinear electrodynamics. This is due to the possible quantum gravity corrections to the linear electrodynamics which originate from superstring theory [16,17]. It has been shown that the BI Lagrangian is not the only nonlinear Lagrangian which can resolve the divergency in the Maxwell's theory. Indeed, other types of nonlinear electrodynamics in the context of gravitational field have been

*asheykhi@shirazu.ac.ir
†zebarjad@susc.ac.ir

introduced, which can also remove the divergence of the electric field at the origin, similar to BI nonlinear electrodynamics. Among them the so-called logarithmic nonlinear (LN) electrodynamics and exponential nonlinear (EN) electrodynamics were considered in [18] and [19], respectively. The former has Lagrangian

$$L_{\mathrm{LN}} = -8\beta^2 \ln\left(1+\frac{F^2}{8\beta^2}\right), \tag{2}$$

while the latter has Lagrangian of the form [19],

$$L_{\mathrm{EN}} = 4\beta^2\left[\exp\left(-\frac{F^2}{4\beta^2}\right)-1\right], \tag{3}$$

where $F^2 = F_{\mu\nu}F^{\mu\nu}$. In our previous works [20,21] we constructed exact black hole solutions of EN electrodynamics in the context of dilaton gravity. In this paper, we would like to consider LN electrodynamics in the framework of dilaton gravity. Because of the presence of both dilaton and nonlinear electrodynamics, the field equations are very complicated, however, we will successfully construct exact analytical black holes solutions of this theory. We shall investigate the effects of the nonlinear electrodynamics as well as dilaton field on the casual structure, physical properties, and thermodynamics of the solutions. Our work differs from [20] in that, we considered in [20] EN electrodynamics in dilaton gravity (ENd), while here we study LN electrodynamics in dilaton theory (LNd). Clearly, the form of their Lagrangian is completely different. Besides, in [20] we only studied spherically symmetric black holes, while here we shall take the topological black holes whose horizon can be a two dimensional surface with positive, zero, or negative curvature. It is worth mentioning that although both solutions ENd and LNd are nonlinear electrodynamics in dilaton gravity, however, they are completely different in the metric function, the electric field expression, and other thermodynamic quantities such as temperature, electric potential, and Smarr formula, as we shall see in this paper. Furthermore, without specifying the explicit form of the matter field Lagrangian (electrodynamics Lagrangian), it is not possible to solve the field equations and find black hole solutions. So one cannot take an arbitrary nonlinear electrodynamics Lagrangian without specifying it. In addition, the number of Lagrangian which have been proposed for the nonlinear electrodynamics in the literature are very limited. The well-known cases are (i) Born-Infeld Lagrangian, (ii) exponential form, (iii) power-law, and (iv) Logarithmic form of the Lagrangian. The first three cases were studied in presence of dilaton field with Liouville-type potentials (see e.g., [20,22,23]). However, the dilatonic version of the case (iv) has not been studied yet and shall be investigated for the first time in the present paper. This study can be useful for future communications in the literature. Clearly in the regime of linear Maxwell field, all nonlinear theories should recover the same results, as expected.

This paper is outlined as follows. In the next section, we introduce the basic field equations and construct a new class of topological black hole solutions of LNd theory with two Liouville-type potentials and general dilaton coupling constant, and investigate their properties. In Sec. III, we study thermodynamics of the obtained solutions and find the conserved and thermodynamics quantities of the topological dilaton black holes. We also check the validity of the first law of thermodynamics on the black hole horizon. In Sec. IV, we calculate heat capacity and Hessian matrix and study thermal stability of the solutions in the canonical and grand canonical ensembles. In Sec. V, we study thermodynamical geometry by introducing the new metric and finding the points in which phase transition happens. We finish our paper with conclusion and discussion in the last section.

II. FIELD EQUATIONS AND SOLUTIONS

Our starting point is the following action in which gravity is coupled to dilaton and LN electrodynamic fields,

$$S = \frac{1}{16\pi}\int d^4x\sqrt{-g}(\mathcal{R} - 2g^{\mu\nu}\partial_\mu\Phi\partial_\nu\Phi - V(\Phi) + L(F,\Phi)), \tag{4}$$

where $\mathcal{R}$ is the Ricci scalar curvature, Φ is the scalar dilaton filed, and $V(\Phi)$ is the potential for Φ. In order to construct the topological dilaton black holes, we choose the dilaton potential in the form of Liouville-type with two terms, namely, [14]

$$V(\Phi) = 2\Lambda_0 e^{2\zeta_0\Phi} + 2\Lambda e^{2\zeta\Phi}, \tag{5}$$

where Λ_0, Λ, ζ_0, and ζ are constants. This kind of potential was previously investigated in the context of Einstein-Maxwell-dilaton (EMd) gravity [4,14] as well as BI-dilaton (BId) black holes [23,24]. We consider the Lagrangian density of LNd theory in the form

$$L(F,\Phi) = -8\beta^2 e^{2\alpha\Phi}\ln\left(1+\frac{F^2e^{-4\alpha\Phi}}{8\beta^2}\right). \tag{6}$$

This is the first time in which Lagrangian (6) is introduced in the literature. In the above expression, α is the dilaton and electromagnetic coupling constant. Expanding Lagrangian (6) for large β, gives

$$L(F,\Phi) = -e^{-2\alpha\Phi}F^2 + \frac{1}{16}\frac{e^{-6\alpha\Phi}F^4}{\beta^2} - \frac{1}{192}\frac{e^{-10\alpha\Phi}F^6}{\beta^4} + O\left(\frac{1}{\beta^6}\right). \tag{7}$$

The motivation for taking the nonlinear Lagrangian in the form of (6), instead of the BId Lagrangian, comes from

the fact that both of them have similar expansion for large β. To see this, let us invoke the BId Lagrangian,

$$L_{\rm BId}(F,\Phi)=4\beta^2 e^{2\alpha\Phi}\left(1-\sqrt{1+\frac{e^{-4\alpha\Phi}F^2}{2\beta^2}}\right). \quad (8)$$

This form for the BId term has been previously investigated by a number of authors [23–30]. For large β, we can expand (8) and arrive at

$$L_{\rm BId}(F,\Phi)=-e^{-2\alpha\Phi}F^2+\frac{e^{-6\alpha\Phi}F^4}{8\beta^2}-\frac{e^{-10\alpha\Phi}F^6}{32\beta^4}+O\left(\frac{1}{\beta^6}\right). \quad (9)$$

We see that both LNd and BId Lagrangian have the same expansion up to a coefficient number in the expanding terms. In the limiting case where $\beta\to\infty$, $L(F,\Phi)$ recovers the standard linear Maxwell Lagrangian coupled to the dilaton field [4]

$$L(F,\Phi)=-e^{-2\alpha\Phi}F^2. \quad (10)$$

For later convenience we set

$$L(F,\Phi)=-8\beta^2 e^{2\alpha\Phi}\mathcal{L}(Y), \quad (11)$$

with definition

$$\mathcal{L}(Y)=\ln(1+Y), \quad (12)$$

$$Y=\frac{F^2 e^{-4\alpha\Phi}}{8\beta^2}. \quad (13)$$

The equations of motion can be derived by varying action (4) with respect to the gravitational field $g_{\mu\nu}$, the dilaton field Φ, and the electromagnetic field A_μ,

$$\mathcal{R}_{\mu\nu}=2\partial_\mu\Phi\partial_\nu\Phi+\frac{1}{2}g_{\mu\nu}V(\Phi)+2e^{-2\alpha\Phi}\partial_Y\mathcal{L}(Y)F_{\mu\eta}F_\nu{}^\eta -4\beta^2 e^{2\alpha\Phi}[2Y\partial_Y\mathcal{L}(Y)-\mathcal{L}(Y)]g_{\mu\nu}, \quad (14)$$

$$\nabla^2\Phi=\frac{1}{4}\frac{\partial V}{\partial\Phi}-4\alpha\beta^2 e^{2\alpha\Phi}[2Y\partial_Y\mathcal{L}(Y)-\mathcal{L}(Y)], \quad (15)$$

$$\nabla_\mu(e^{-2\alpha\Phi}\partial_Y\mathcal{L}(Y)F^{\mu\nu})=0. \quad (16)$$

For $\beta^2\to\infty$ we have $\mathcal{L}(Y)=Y$, and the system of equations (14)–(16) reduce to the well-known equations of EMd gravity [4–6,14].

Our aim in this paper is to construct topological solutions of the above field equations. The most general of such metric can be written in the form

$$ds^2=-f(r)dt^2+\frac{dr^2}{f(r)}+r^2R^2(r)d\Omega_k^2, \quad (17)$$

where $f(r)$ and $R(r)$ are functions of r which should be determined, and $d\Omega_k^2$ is the line element of a two-dimensional hypersurface Σ with constant curvature,

$$d\Omega_k^2=\begin{cases}d\theta^2+\sin^2\theta d\phi^2, & \text{for } k=1,\\ d\theta^2+\theta^2 d\phi^2, & \text{for } k=0,\\ d\theta^2+\sinh^2\theta d\phi^2, & \text{for } k=-1.\end{cases} \quad (18)$$

For $k=1$, the topology of the event horizon is the two-sphere S^2, and the spacetime has the topology $R^2\times S^2$. For $k=0$, the topology of the event horizon is that of a torus and the spacetime has the topology $R^2\times T^2$. For $k=-1$, the surface Σ is a 2-dimensional hypersurface H^2 with constant negative curvature. In this case the topology of spacetime is $R^2\times H^2$. The additional function $R(r)$ is introduced in the metric due to the presence of the new degree of freedom associated with the dilation field in the equations of motion.

First of all, we integrate the electromagnetic field equation (16). For this purpose we assume all the components of $F_{\mu\nu}$ are zero except F_{tr}:

$$F_{tr}=\frac{2qe^{2\alpha\Phi}}{r^2R^2(r)}\left(1+\sqrt{1+\frac{q^2}{\beta^2r^4R^4(r)}}\right)^{-1}, \quad (19)$$

where q is an integration constant which is related to the electric charge of the topological black holes. From the Gauss law we can obtain the charge of the solution as,

$$Q=\frac{1}{4\pi}\int e^{-2\alpha\Phi*}Fd\Omega_k=\frac{q\omega}{4\pi}, \quad (20)$$

where ω represents the area of the constant hypersurface Σ. For large β, the electric field reduces to

$$F_{tr}=\frac{qe^{2\alpha\Phi}}{r^2R^2(r)}-\frac{1}{4\beta^2}\frac{q^3e^{2\alpha\Phi}}{r^6R^6(r)}+O\left(\frac{1}{\beta^4}\right). \quad (21)$$

The first term in (21) is the electric field of EMd black holes [14]. The second term is the leading order nonlinear correction term and in the case of $\beta\to\infty$ it vanishes. On the other hand, in the absence of the dilaton field the electric field reduces to [31]

$$F_{tr}=\frac{2q}{r^2}\left(1+\sqrt{1+\frac{q^2}{\beta^2r^4}}\right)^{-1}. \quad (22)$$

We have three unknown functions $f(r)$, $R(r)$, and $\Phi(r)$ in equations (14) and (15). The suitable ansatz for solving the system of equations is [8]

$$R(r)=e^{\alpha\Phi}. \quad (23)$$

This is a reasonable ansatz, since in the absence of nontrivial dilaton ($\alpha=0$), it leads to $R(r)=1$, as expected.

After substituting (17), (19), and (23) into the field equation (14), we find that subtracting (tt) and (rr)-components of this equation leads to the following differential equation for the dilaton field,

$$r\alpha\Phi'' + 2\alpha\Phi' + r(\alpha^2+1)\Phi'^2 = 0. \tag{24}$$

The above equation has the following solution

$$\Phi(r) = \frac{\alpha}{\alpha^2+1}\ln\left(c + \frac{b}{r}\right), \tag{25}$$

where c and b are integration constants. The other components of the field equation (14), gives

$$\begin{aligned} f(r) = &-k\frac{(\alpha^2+1)}{(\alpha^2-1)}b^{-\gamma}r^{\gamma} - \frac{m}{r^{1-\gamma}} + \frac{(\Lambda-4\beta^2)(\alpha^2+1)^2}{\alpha^2-3}b^{\gamma}r^{2-\gamma} \\ &-4\beta^2 b^{\gamma}(\alpha^2+1)r^{\gamma-1} \\ &\times\int r^{2-2\gamma}\left\{\sqrt{1+\eta} - \ln\left(\frac{\eta}{2}\right) + \ln\left(-1+\sqrt{1+\eta}\right)\right\}dr, \end{aligned} \tag{26}$$

where m is the mass parameter, $\gamma = 2\alpha^2/(1+\alpha^2)$, and

$$\eta = \frac{q^2 b^{-2\gamma}}{\beta^2 r^{4-2\gamma}}. \tag{27}$$

We find that solutions (25) and (26) will fully satisfy all components of the field equations (14)–(15) provided we choose, $c = 0$, $\zeta_0 = 1/\alpha$, $\zeta = \alpha$, and

$$\Lambda_0 = k\frac{b^{-2}\alpha^2}{\alpha^2-1}. \tag{28}$$

We see that either for $k = 0$ or $\alpha = 0$, the term proportional to Λ_0 in the Liouville potentials (5) vanishes. This implies that in the case of flat horizon we can take Liouville potentials with only one term [30]. Note that Λ still remains as a free parameter which plays the role of the cosmological constant in the absence of the dilaton field where the potential reduces $V(\Phi) \to 2\Lambda$. Thus, one may redefine it as usual, $\Lambda = -3/l^2$, where l is a constant with dimension of length.

We use the Mathematica software to perform the integral of Eq. (26). After time-consuming calculations, we find

$$\begin{aligned} f(r) = &-k\frac{(\alpha^2+1)}{(\alpha^2-1)}b^{-\gamma}r^{\gamma} - \frac{m}{r^{1-\gamma}} + \frac{(\Lambda-4\beta^2)(\alpha^2+1)^2}{\alpha^2-3}b^{\gamma}r^{2-\gamma} \\ &+\frac{8\beta^2(\alpha^2+1)^2}{(\alpha^2-3)^2}b^{\gamma}r^{2-\gamma}\left\{1 - {}_2F_1\left(\left[-\frac{1}{2},\frac{\alpha^2-3}{4}\right],\left[\frac{\alpha^2+1}{4}\right],-\eta\right)\right\} \\ &+\frac{4\beta^2(\alpha^2+1)^2}{(\alpha^2-3)}b^{\gamma}r^{2-\gamma}\left\{\sqrt{1+\eta} - \ln\left(\frac{\eta}{2}\right) + \ln\left(-1+\sqrt{1+\eta}\right)\right\}. \end{aligned} \tag{29}$$

When $\alpha = 0 = \gamma$, our solution can reproduce the asymptotically AdS topological black holes coupled to logarithmic nonlinear electrodynamics [31]. On the other hand, we can expand $f(r)$ for large β. The result is

$$f(r) = -k\frac{(\alpha^2+1)}{(\alpha^2-1)}b^{-\gamma}r^{\gamma} - \frac{m}{r^{1-\gamma}} + \frac{\Lambda(\alpha^2+1)^2}{\alpha^2-3}b^{\gamma}r^{2-\gamma} + \frac{q^2(\alpha^2+1)b^{-\gamma}}{r^{2-\gamma}} - \frac{q^4(\alpha^2+1)^2}{8\beta^2(\alpha^2+5)}\frac{b^{-3\gamma}}{r^{6-3\gamma}} + O\left(\frac{1}{\beta^4}\right). \tag{30}$$

This is exactly the result obtained for EMd black holes in the limit $\beta \to \infty$ [14]. The last term in (30) is the leading order correction term to the topological black holes of EMd gravity and incorporate the effect of the nonlinear electrodynamics into the metric function. It is also interesting to see (30) in the special case where $\alpha = \gamma = 0$. In this case our solution reduces to

$$f(r) = k - \frac{m}{r} + \frac{r^2}{l^2} + \frac{q^2}{r^2} - \frac{1}{40\beta^2}\frac{q^4}{r^6} + O\left(\frac{1}{\beta^4}\right), \tag{31}$$

which describes an asymptotically AdS topological black hole with a positive, zero, or negative constant curvature hypersurface in the $\beta \to \infty$ limit [32,33]. Again, the last term in the right-hand side of (31) is the leading nonlinear correction term to the topological black holes in the large β limit.

A. Physical properties of solutions

Now we back to the electric field obtained in (19). In order to study the behavior of the electric field, we combine Eqs. (23) and (25) with (19). We find

$$F_{tr} = E(r) = \frac{2q}{r^2}\left(1 + \sqrt{1 + \frac{q^2}{\beta^2 b^{2\gamma} r^{4-2\gamma}}}\right)^{-1}. \tag{32}$$

Let us remember that the electric field in the case of BId black holes is given by [24]

TABLE I. $E(r)$ for LNd versus r for $\beta = 2$, $q = 2$, and $b = 1$ and different values of α.

$r = 10^3$		10^2	10^1	10^{-1}	10^{-10}	10^{-1000}
$\alpha = 0.0$	2×10^{-6}	2×10^{-4}	2×10^{-2}	3.960	4.0	4.0
$\alpha = 0.4$	2×10^{-6}	2×10^{-4}	2×10^{-2}	4.7	23	10^{77}
$\alpha = 0.8$	2×10^{-6}	2×10^{-4}	2×10^{-2}	7.4	2×10^3	10^{277}

$$F_{tr}^{\mathrm{BId}} = \frac{q}{r^2}\left(1 + \frac{q^2}{\beta^2 b^{2\gamma} r^{4-2\gamma}}\right)^{-1/2}. \tag{33}$$

Expanding for large β, we arrive at

$$E(r) = \frac{q}{r^2} - \frac{q^3 b^{-2\gamma}}{4\beta^2 r^{6-2\gamma}} + O\left(\frac{1}{\beta^4}\right). \tag{34}$$

In order to analyze the behavior of $E(r)$, we choose $b = 1$, and $\alpha = \sqrt{2}$ ($\gamma = 4/3$). For these values of the parameters, we have

$$E(r) = \frac{q}{r^2} - \frac{q^3}{4\beta^2 r^{10/3}} + O\left(\frac{1}{\beta^4}\right). \tag{35}$$

From Eq. (35) we see that in the presence of the dilaton field, the electric field diverges as $r \to 0$. The values of the electric field, *near the origin*, for different values of the dilaton coupling parameter, α, is summarized in Table I.

To have better understanding on the behavior of $E(r)$, we have also plotted Figs. 1–6. Table I shows that with increasing α, the value of the electric field increases *near the origin* where $r \to 0$. On the other hand, Figs. 1–3 show that far from the black holes, where $r \to \infty$, the electric field goes to zero, independent of the model parameters. This is an expected result, since in this case the effects of nonlinearity disappear. Figure 1 shows that for topological LNd black holes, and in the absence of the dilaton field ($\alpha = 0$), the electric field has a finite value at $r = 0$, while as soon as the dilaton field is taken into account ($\alpha > 0$), the electric field diverges as $r \to 0$. Besides, the divergency of the electric field *near the origin* increases with increasing the dilaton coupling parameter α. In Fig. 2, we have compared the behavior of $E(r)$ near the origin for EMd, LNd, and BId, and for $\alpha = 0.4$. From this figure we see that the divergency of the electric field near the origin for LNd is weaker than EMd and stronger than BId. Finally, in Fig. 3 we have shown the effects of the nonlinear parameter β on the behavior of the electric field. From this figure we see

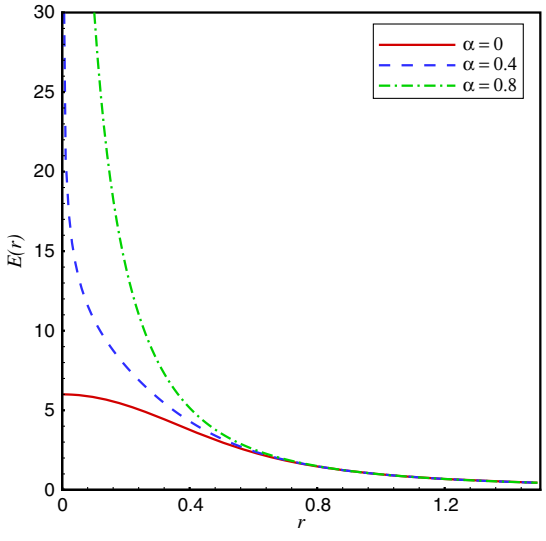

FIG. 1 (color online). The behavior of the electric field $E(r)$ of LNd topological black holes versus r for $\beta = 3$, $b = 1$, and $q = 1$.

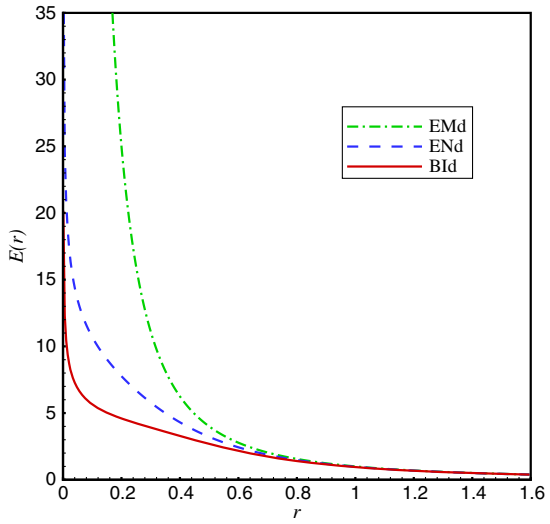

FIG. 2 (color online). The behavior of the electric field $E(r)$ versus r for $b = 1$, $\beta = 3$, $\alpha = 0.4$, and $q = 1$.

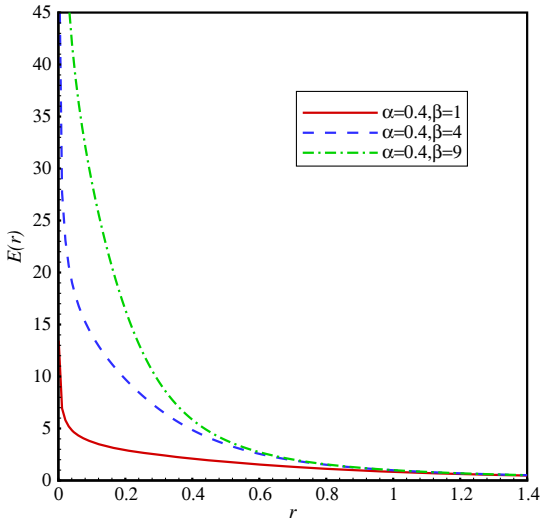

FIG. 3 (color online). The behavior of the electric field $E(r)$ of LNd topological black holes versus r for $b = 1$ and $q = 1$.

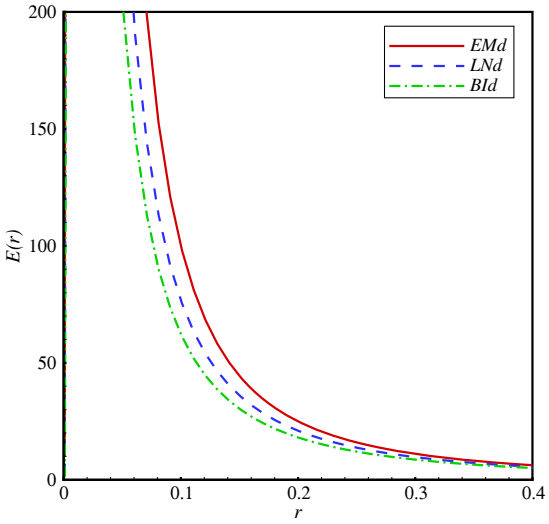

FIG. 4 (color online). The behavior of the electric field $E(r)$ versus r for $b = 1 = q$, $\beta = 2 = \alpha$.

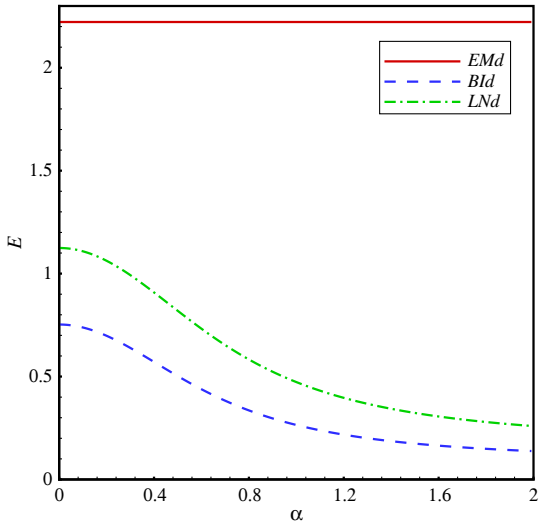

FIG. 6 (color online). The behavior of the electric field $E(r)$ versus α for the case $r > b$. The parameters are fixed as $b = 0.1$, $\beta = .8$, $r = 0.3$, and $q = 0.2$.

that with increasing β, the electric field diverges *near the origin*. This is an expected result, since for large β, our solution reduces to topological black holes of EMd theory [14]. Figure 4 shows that for $r < b$ and large value of α, the electric field of BId and LNd have a behavior similar to linear EMd. To see this better, we have plotted in Fig. 5 the behavior of the electric field versus α for fixed r in case $r < b$. This figure shows that in this case, with increasing α, the electric field of BId and LNd black holes approaches to the electric field of EMd black holes. Note that this behavior can be seen only for $r < b$ and in the case of $r > b$, the behavior completely differs, as shown in Fig. 6.

Next, we study the casual structure of the solutions and check whether there is or is not the curvature singularities

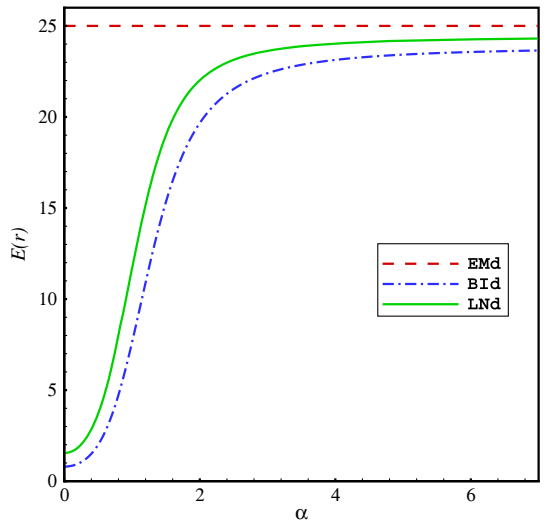

FIG. 5 (color online). The behavior of the electric field $E(r)$ versus α for the case $r < b$. The parameters are fixed as $b = 2$, $\beta = .8$, $r = 0.2$, and $q = 1$.

and horizons. Our calculations show that $R_{\mu\nu\lambda\kappa}R^{\mu\nu\lambda\kappa} \to \infty$ as $r \to 0$. This implies that our spacetime has an essential singularity located at $r = 0$. Now, we explore the asymptotic behavior of the solutions. Expanding the metric function $f(r)$ for $r \to \infty$ limit, and $\gamma > 1$ or $(\alpha > 1)$, gives

$$\lim_{r\longrightarrow\infty} f(r) = -k\frac{(\alpha^2+1)}{(\alpha^2-1)}b^{-\gamma}r^{\gamma} - \frac{m}{r^{1-\gamma}} + \frac{\Lambda(\alpha^2+1)^2}{(\alpha^2-3)}b^{\gamma}r^{2-\gamma}. \tag{36}$$

Note that from its definition we have always $\gamma < 2$. On the other hand, for $\gamma < 1$ or $(\alpha < 1)$, it gives

$$\lim_{r\longrightarrow\infty} f(r) = -k\frac{(\alpha^2+1)}{(\alpha^2-1)}b^{-\gamma}r^{\gamma} + \frac{\Lambda(\alpha^2+1)^2}{(\alpha^2-3)}b^{\gamma}r^{2-\gamma}. \tag{37}$$

Let us note that in the absence of the dilaton field $(\alpha = 0 = \gamma)$, the metric function becomes

$$\lim_{r\longrightarrow\infty} f(r) = k + \frac{r^2}{l^2}, \tag{38}$$

which describes an asymptotically AdS spacetimes. However, as one can see from Eqs. (36) and (37), in the presence of the dilaton field the asymptotic behavior of the metric is neither flat nor (A)dS. For example, taking $\alpha = \sqrt{2}$, and $b = 1$, we have

$$\lim_{r\longrightarrow\infty} f(r) = -3kr^{4/3} - mr^{1/3} - 9\Lambda r^{2/3}. \tag{39}$$

Clearly, the asymptotic behavior of (39) is not (A)dS. Indeed, it has been shown that no dilaton dS or AdS black hole solutions exists with the presence of only one or two

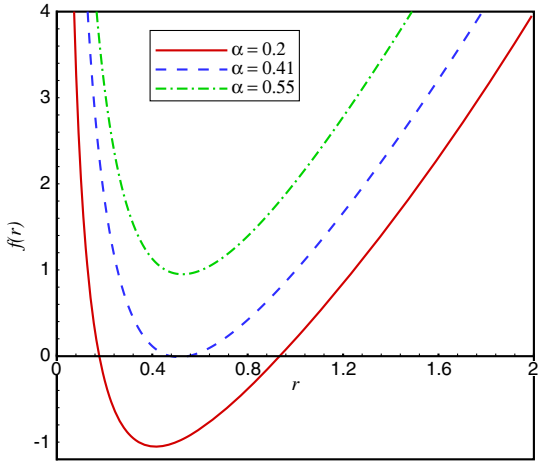

FIG. 7 (color online). $f(r)$ versus r for $k = 1$, $q = 1$, $\beta = 1$, and $m = 3$.

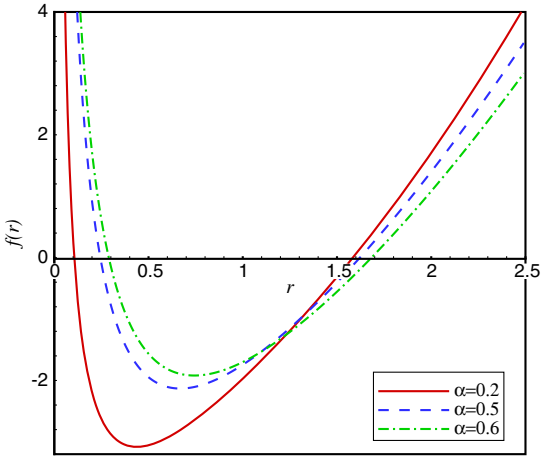

FIG. 9 (color online). $f(r)$ versus r for $k = -1$, $q = 1$, $\beta = 1$, and $m = 3$.

Liouville-type dilaton potentials [2]. In the presence of one or two Liouville-type potentials, black hole spacetimes which are neither asymptotically flat nor (A)dS have been explored by many authors (see, e.g., [2–14]). Here we see that a similar situation also holds in the case of dilaton black holes coupled to logarithmic nonlinear electrodynamics. It is important to note that this asymptotic behavior is not due to the nonlinear nature of the electrodynamic field, since as $r \to \infty$ the effects of the nonlinearity disappear. This is due to the fact that, $r \to \infty$ limit corresponds to $\beta^2 \to \infty$, and in this case F_{tr} as well as the metric functions $f(r)$ restore the results of topological EMd with unusual asymptotic [14]. Furthermore, from the dilaton field (25) we see that as $r \to \infty$, the dilaton field does not vanish, while in the case of asymptotic flat or (A) dS we expect to have $\lim_{r\longrightarrow\infty}\Phi(r) = 0$. From the above arguments we conclude that the asymptotic behavior of the obtained solutions is neither flat nor (A)dS.

It is worth mentioning that in $k = \pm 1$ cases this solution does not exist for the string case where $\alpha = 1$. As one can see from Eq. (29), the solution is also ill-defined for $\alpha = \sqrt{3}$ independent of the curvature parameter k. Now, we search for the horizons of spacetime. Although, in principle, the casual structure of the spacetime can be obtained by finding the roots of $f(r) = 0$, but because of the nature of the dilaton and nonlinear electrodynamic fields in (29), it is not possible to find analytically the location of the horizons. However, we can plot the function $f(r)$ versus r for different model parameters (see Figs. 7–13). For simplicity, in these figures, we set $l = b = 1$. Figure 7 and 8 show that, in the case of $k = 0, 1$, for fixed value of the other parameters, the number of horizons decreases with increasing α, while for the same value of the parameters and $k = -1$, our black holes have always two inner and outer horizons (Fig. 9). One can see from Fig. 10 that, for fixed value of the parameters, the number of horizons also

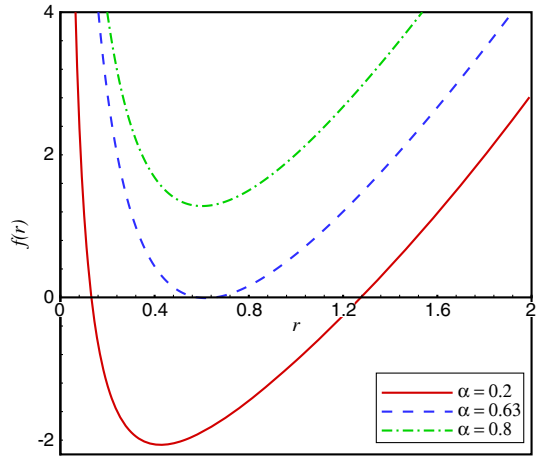

FIG. 8 (color online). $f(r)$ versus r for $k = 0$, $q = 1$, $\beta = 1$, and $m = 3$.

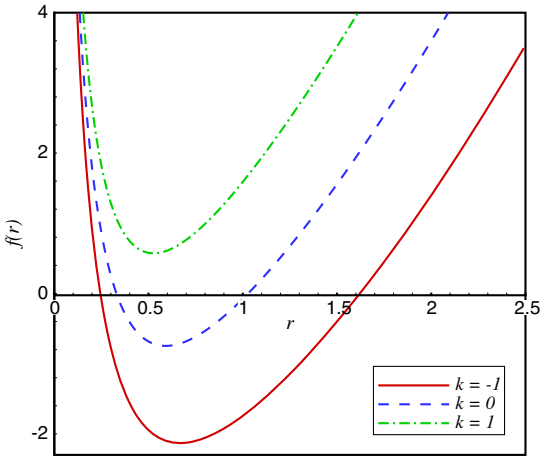

FIG. 10 (color online). $f(r)$ versus r for $\alpha = 0.5$, $q = 1$, $\beta = 1$, and $m = 3$.

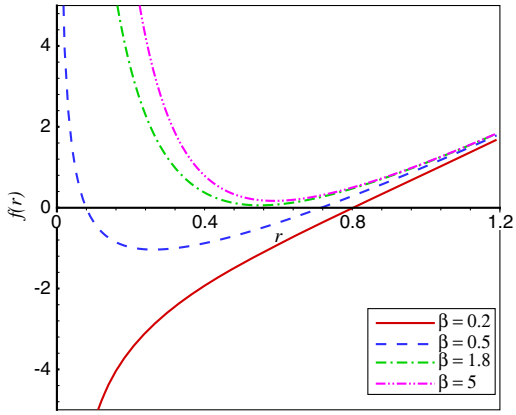

FIG. 11 (color online). $f(r)$ versus r for $\alpha = 0.5$, $k = 1$, $q = 1$, and $m = 3.5$.

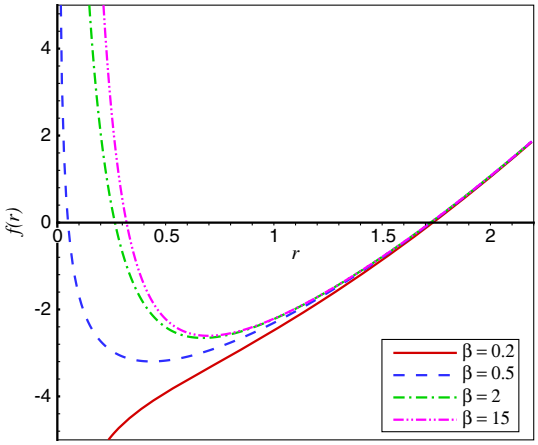

FIG. 13 (color online). $f(r)$ versus r for $\alpha = 0.5$, $k = -1$, $q = 1$, and $m = 3.5$.

depends on the horizon curvature k. The behavior of $f(r)$ versus r for different value of the nonlinear parameter is shown in Figs. 11–13. Figure 11 shows that in the case of $k = 1$ and fixed value of m, α, and q, there is a minimum (extreme) value for the nonlinear parameter $\beta_{\min}(\beta_{\text{ext}})$, for which we have black hole with a nonextreme horizon provided $\beta \leq \beta_{\min}$ (red curve), black hole with two horizons for $\beta_{\min} < \beta < \beta_{\text{ext}}$ (blue curve), black hole with an extreme horizon for $\beta = \beta_{\text{ext}}$ (green curve), and naked singularity for $\beta > \beta_{\text{ext}}$ (purple curve). Clearly, $\beta_{\min}$ and β_{ext} depend on the other parameters of the model. On the other hand, in the case of $k = 0, 1$ and for the same values of the parameters, we have a nonextreme black holes with one horizon for $\beta \leq \beta_{\min}$ and black holes with two horizon for $\beta > \beta_{\min}$ (Figs. 12 and 13).

In summary, Figs. 7–13 show that the obtained solutions in (29) describe a nonlinear topological dilaton black hole with one or two horizons, or a naked singularity depending on the values of the parameters.

In order to get better understanding of the nature of the horizons, we plot in Figs. 14–17, the mass parameter m as a function of the horizon radius r_h for different model parameters. Using the fact that $f(r_h) = 0$, we can obtain the mass parameter in terms of the horizon radius,

$$m(r_h) = -\frac{(\alpha^2+1)}{(\alpha^2-1)} b^{-\gamma} r_h + \frac{(\Lambda - 4\beta^2)(\alpha^2+1)^2}{\alpha^2-3} b^{\gamma} r_h^{3-2\gamma} + \frac{8\beta^2(\alpha^2+1)^2}{(\alpha^2-3)^2} b^{\gamma} r_h^{3-2\gamma} \left\{ 1 - {}_2F_1\left(\left[\frac{-1}{2}, \frac{\alpha^2-3}{4} \right], \left[\frac{\alpha^2+1}{4} \right], -\eta_h \right) \right\}$$
$$+ \frac{4\beta^2(\alpha^2+1)^2}{(\alpha^2-3)} b^{\gamma} r_h^{3-2\gamma} \left\{ \sqrt{1+\eta_h} - \ln\left(\frac{\eta_h}{2}\right) + \ln\left(-1+\sqrt{1+\eta_h}\right) \right\}, \tag{40}$$

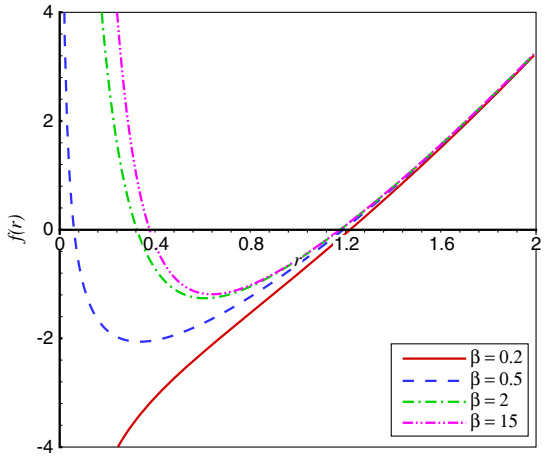

FIG. 12 (color online). $f(r)$ versus r for $\alpha = 0.5$, $k = 0$, $q = 1$, and $m = 3.5$.

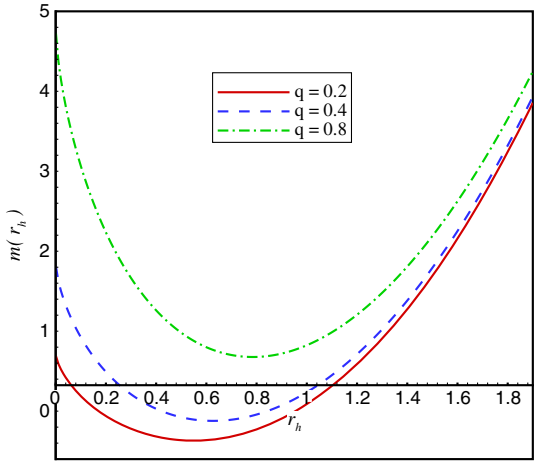

FIG. 14 (color online). $m(r_h)$ versus r_h for $\alpha = 0.5$, $k = -1$, and $\beta = 1$.

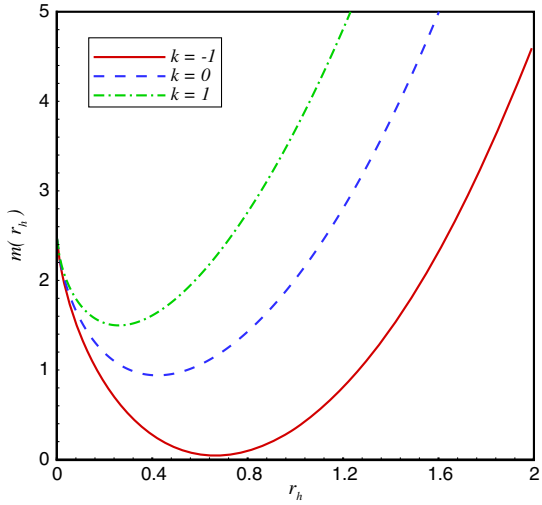

FIG. 15 (color online). $m(r_h)$ versus r_h for $\alpha = 0.5$, $q = 0.5$, and $\beta = 1$.

where $\eta_h = \eta(r = r_h)$. For simplicity, we set $l = b = 1$. These figures show that for a given value of α, the number of horizons depend on the choice of the value of the mass parameter m. We see that, up to a certain value of the mass parameter m, there are two horizons, and as we decrease m further, the two horizons meet. In this case we get an extremal black hole (see the next section). Besides, in the case $k = -1$ and small q, our solution has strange properties. Figure 14 shows that in this case the mass parameter may become negative for a small value of the charge parameter, however one still has a topological black hole solution with negative curvature horizons. It was argued that this kind of black hole with negative mass can also be formed as a result of gravitational collapse [34]. From Fig. 15 and 16 we see that in the limit $r_h \to 0$ we have a nonzero value for the mass parameter m. This is in contrast to the Schwarzschild black holes in which mass parameter

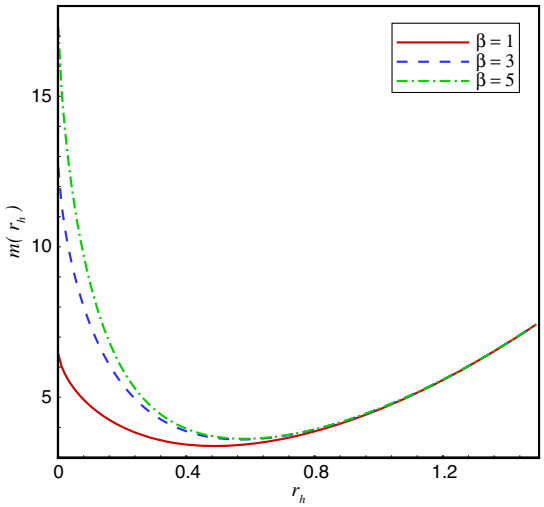

FIG. 16 (color online). $m(r_h)$ versus r_h for $\alpha = 0.5$, $k = 1$, and $q = 1$.

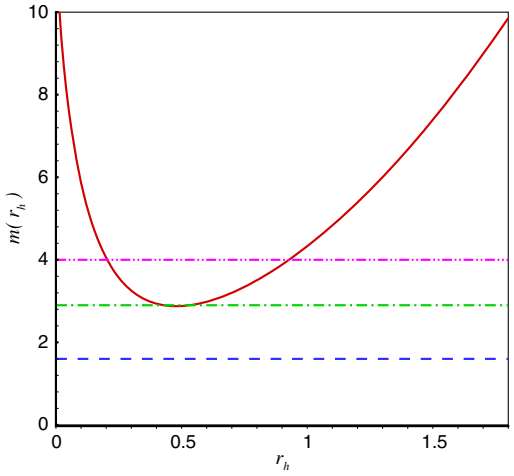

FIG. 17 (color online). The mass parameter m versus r_h for $k = 1$, $\alpha = 0.52$, $\beta = 4$, and $q = 0.8$. $m < m_{\text{ext}}$ (blue line), $m = m_{\text{ext}}$ (green line), $m > m_{\text{ext}}$ (purple line).

goes to zero as $r_h \to 0$. This is due to the effect of the nonlinearity of the electrodynamic field and in the case of $q = 0$, the mass parameter m goes to zero as $r_h \to 0$.

III. THERMODYNAMICS OF SOLUTIONS

In this section we would like to investigate thermodynamical properties of the topological LNd black holes. There are several ways for calculating the mass of the black holes. For example, for an asymptotically AdS solution one can use the counterterm method inspired by AdS/CFT correspondence [35,36]. Another way for calculating the mass is through the use of the substraction method of Brown and York [37]. Such a procedure causes the resulting physical quantities to depend on the choice of reference background. In our case, due to the presence of the nontrivial dilaton field, the asymptotic behavior of the solutions are neither flat nor (A)dS, therefore we use the reference background metric and calculate the mass. Using the modified BY method [38], the mass of the topological dilaton black holes is obtained as [24]

$$M = \frac{b^{\gamma} m \omega}{8\pi(\alpha^2 + 1)}. \tag{41}$$

The Hawking temperature of the black hole on the outer horizon r_+, may be obtained through the use of the definition of surface gravity [19]

$$T_+ = \frac{\kappa}{2\pi} = \frac{1}{2\pi}\sqrt{-\frac{1}{2}(\nabla_\mu \chi_\nu)(\nabla^\mu \chi^\nu)}, \tag{42}$$

where κ is the surface gravity and $\chi = \partial/\partial t$ is the null killing vector of the horizon. Taking $\chi^\nu = (-1, 0, 0, 0)$, we have $\chi_\nu = (f(r_+), 0, 0, 0)$ and hence $(\nabla_\mu \chi_\nu)(\nabla^\mu \chi^\nu) = -\frac{1}{2}[f'(r_+)]^2$ which leads to

$$\kappa = \sqrt{-\frac{1}{2}(\nabla_\mu \chi_\nu)(\nabla_\mu \chi_\nu)} = \frac{1}{2}\left(\frac{df(r)}{dr}\right)_{r=r_+}. \tag{43}$$

Thus, the temperature is obtained as

$$T_+ = \frac{f'(r_+)}{4\pi} = -2k\frac{b^{-\gamma} r_+^{\gamma-1}}{4\pi} - \frac{m(\alpha^2-3)}{4\pi(\alpha^2+1)} r_+^{\gamma-2} + \frac{8\beta^2(\alpha^2+1)}{4\pi(\alpha^2-3)} b^{\gamma} r_+^{1-\gamma}\left(1 - \frac{1}{\sqrt{1+\eta_+}}\right)$$
$$+ \frac{8q^2}{4\pi(\alpha^2-3)} b^{-\gamma} r_+^{\gamma-3}\left\{2_2F_1\left(\left[\frac{1}{2}, \frac{\alpha^2+1}{4}\right], \left[\frac{\alpha^2+5}{4}\right], -\eta_+\right) - \frac{\alpha^2+1}{\sqrt{1+\eta_+}}\right\}, \tag{44}$$

where $\eta_+ = \eta(r = r_+)$ and we have used $f(r_+) = 0$ for deleting Λ. We have plotted T versus r_+ in Figs. 18–21. It can be easily seen that for large value of r_+, the temperature tends to a constant independent of the model parameters, while for small values of r_+, the temperature may be negative ($T < 0$). In this case we encounter a naked singularity. The temperature of the black hole is zero in the case of the extremal black hole. In this case the mass parameter of the extremal black holes can be obtained through Eq. $T_+(r = r_{\rm ext}) = 0$,

$$m_{\rm ext} = -2k\frac{(\alpha^2+1)}{\alpha^2-3} b^{-\gamma} r_{\rm ext} + \frac{8q_{\rm ext}^2(\alpha^2+1)b^{-\gamma}}{r_{\rm ext}(\alpha^2-3)^2}\left(2 \times {}_2F_1\left(\left[\frac{1}{2}, \frac{\alpha^2+1}{4}\right], \left[\frac{\alpha^2+5}{4}\right], -\eta_{\rm ext}\right) - \frac{\alpha^2+1}{\sqrt{1+\eta_{\rm ext}}}\right)$$
$$+ \frac{8\beta^2(\alpha^2+1)^2}{(\alpha^2-3)^2} b^{\gamma} r_{\rm ext}^{3-2\gamma}\left(1 - \frac{1}{\sqrt{1+\eta_{\rm ext}}}\right), \tag{45}$$

where $\eta_{\rm ext} = \eta(r = r_{\rm ext})$. From Fig. 17 we see that if we solve equation $m = $ const. for r_h, we can distinguish three cases depending on the value of m. For $m > m_{\rm ext}$, there exist two value for $r_h = r_\pm$ and thus we have two horizons, for $m = m_{\rm ext}$ the two horizons meet. In this case we encounter an extremal black hole with zero temperature. Besides, for $m < m_{\rm ext}$ there is no horizon. In summary, the metric of Eqs. (61) and (29) can describe a topological dilaton black hole with inner and outer event horizons located at r_- and r_+, provided $m > m_{\rm ext}$, an extreme topological black hole in the case of $m = m_{\rm ext}$, and a naked singularity if $m < m_{\rm ext}$.

It is worth noting that for $\beta \to \infty$, we obtain the temperature of topological dilaton black holes of EMd gravity [14]

$$T_+ = -k\frac{b^{-\gamma} r_+^{\gamma-1}}{2\pi} - \frac{m(\alpha^2-3)}{4\pi(\alpha^2+1)} r_+^{\gamma-2} - \frac{q^2 b^{-\gamma}}{\pi r_+^{3-\gamma}} + O\left(\frac{1}{\beta^2}\right). \tag{46}$$

We employ the area law to obtain the entropy of the topological black holes. It is easy to show that

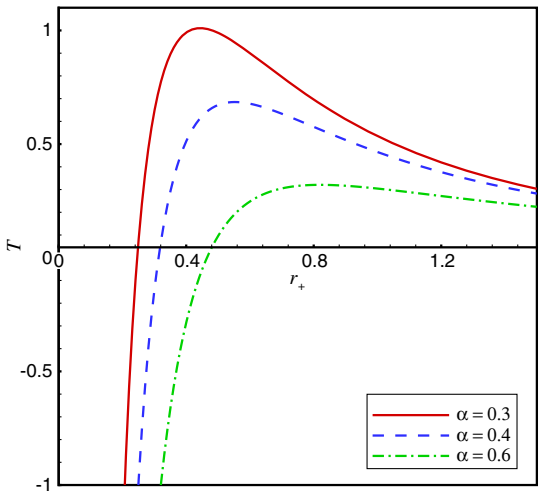

FIG. 18 (color online). T versus r_+ for $\beta = 2$, $k = 0$, $m = 4$, and $q = 1$.

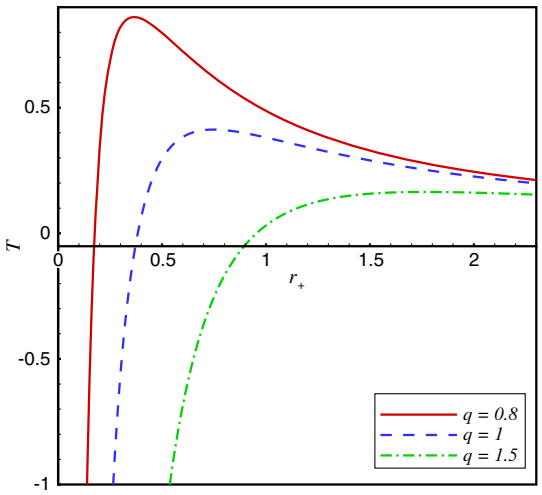

FIG. 19 (color online). T versus r_+ for $\alpha = 0.5$, $k = -1$, $m = 3$, and $\beta = 1$.

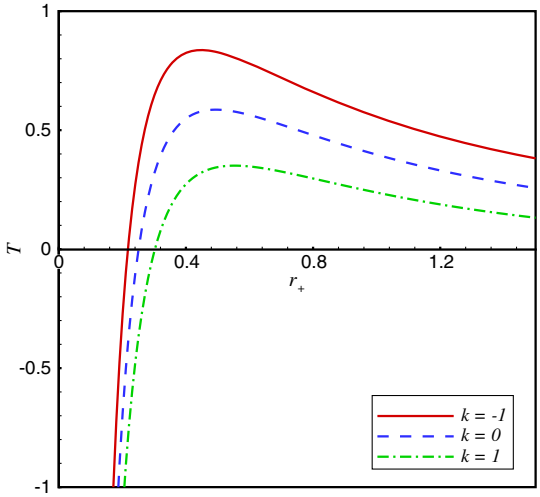

FIG. 20 (color online). T versus r_+ for $\alpha = 0.5$, $\beta = 1$, $m = 4$, and $q = 1$.

$$S = \frac{A}{4} = \frac{b^{\gamma} r_+^{2-\gamma} \omega}{4}. \tag{47}$$

The gauge potential A_t corresponding to the electromagnetic field (34) can be obtained through relation $F_{\mu\nu} = \partial_\mu A_\nu - \partial_\nu A_\mu$. Since our solution is static, the gauge potential is only a function of r. From $F_{tr} = \partial_t A_r - \partial_r A_t$ with $\partial_t A_r = 0$ we have

$$F_{tr} + \partial_r A_t(r) = 0, \tag{48}$$

and hence the gauge potential A_t can be derived as

$$A_t(r) = -\int F_{tr} dr = -\int \frac{2q}{r^2}\left(1 + \sqrt{1 + \frac{q^2}{\beta^2 b^{2\gamma} r^{4-2\gamma}}}\right)^{-1} dr. \tag{49}$$

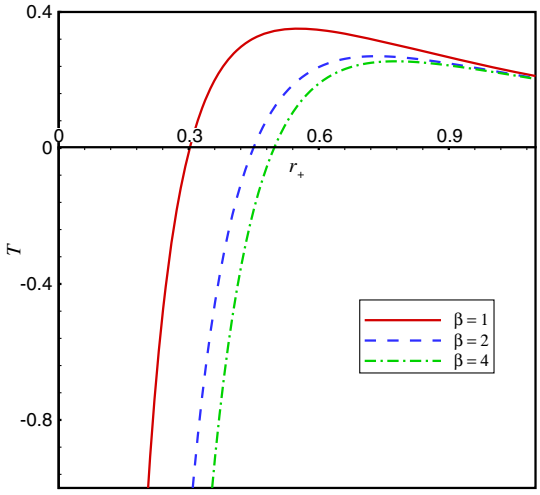

FIG. 21 (color online). T versus r_+ for $\alpha = 0.5$, $k = 1$, $m = 4$, and $q = 1$.

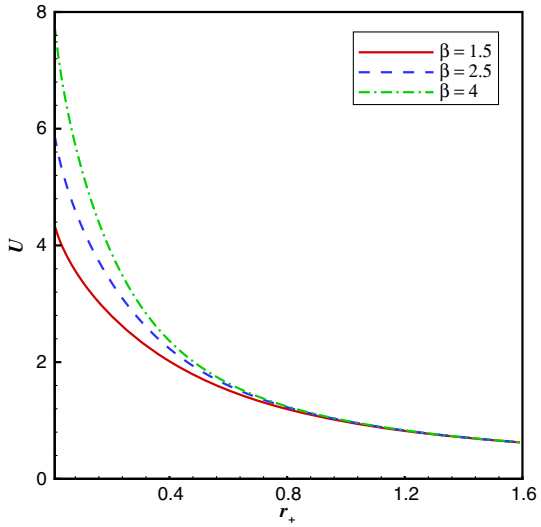

FIG. 22 (color online). $U(r_+)$ versus r_+ for $\alpha = 0.5$ and $q = 1 = b$.

Integrating yields

$$A_t = \frac{q}{r} \times {}_3F_2\left(\left[\frac{1}{2}, 1, \frac{\alpha^2+1}{4}\right], \left[2, \frac{\alpha^2+5}{4}\right], -\eta\right), \tag{50}$$

where ${}_3F_2$ is the hypergeometric function and we have set the constant of integration equal to zero, since for $r \to \infty$ or $\beta \to \infty$, Eq. (50) should restore the well-known relation $A_t = q/r$. Using the standard definition for the electric potential U [30],

$$U = A_\nu \chi^\nu|_{r\to\infty} - A_\nu \chi^\nu|_{r=r_+}, \tag{51}$$

we find

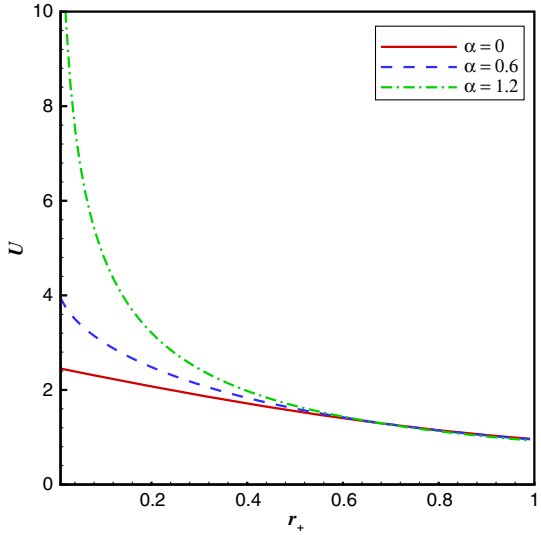

FIG. 23 (color online). $U(r_+)$ versus r_+ for $q = 1 = b$ and $\beta = 1$.

$$U = \frac{q}{r_+} \times {}_3F_2\left(\left[\frac{1}{2}, 1, \frac{\alpha^2+1}{4}\right], \left[2, \frac{\alpha^2+5}{4}\right], -\eta_+\right). \quad (52)$$

Expanding for large β, we get

$$U = \frac{q}{r_+} - \frac{b^{-2\gamma}(\alpha^2+1)}{4\beta^2(\alpha^2+5)} \frac{q^3}{r_+^{5-2\gamma}} + O\left(\frac{1}{\beta^4}\right). \quad (53)$$

The behavior of the electric potential U as a function of horizon radius r_+ is shown in Figs. 22 and 23. From this figures we see that the electric potential can be finite as $r_+ \to 0$, depending on the model parameters, and goes to zero as $r_+ \to \infty$, independent of the model parameters. Again, we see that the divergency of U, for small r_+, increases with increasing α and β.

Having the conserved and thermodynamic quantities at hand, we are in the position to check the validity of the first law of thermodynamics on the horizon for the topological dilaton black holes. For this purpose, we first obtain the mass M as a function of extensive quantities S and Q. Combining expressions for the charge, the mass, and the entropy given in Eqs. (20), (41), and (47), and using the fact that $f(r_+) = 0$, we obtain a Smarr-type formula as

$$\begin{aligned} M(S,Q) = & -k\frac{b^{-\alpha^2}(4S)^{(\alpha^2+1)/2}}{8\pi(\alpha^2-1)} + \frac{\Lambda(\alpha^2+1)b^{\alpha^2}(4S)^{(3-\alpha^2)/2}}{8\pi(\alpha^2-3)} - \frac{\beta^2(\alpha^2+1)(\alpha^2-5)b^{\alpha^2}(4S)^{(3-\alpha^2)/2}}{2\pi(\alpha^2-3)^2} \\ & - \frac{\beta^2(\alpha^2+1)b^{\alpha^2}(4S)^{(3-\alpha^2)/2}}{\pi(\alpha^2-3)^2} {}_2F_1\left(\left[\frac{-1}{2}, \frac{\alpha^2-3}{4}\right], \left[\frac{\alpha^2+1}{4}\right], -\zeta\right) \\ & + \frac{\beta^2(\alpha^2+1)b^{\alpha^2}}{2\pi(\alpha^2-3)}(4S)^{(3-\alpha^2)/2}\left\{\sqrt{1+\zeta} - \ln\left(\frac{\zeta}{2}\right) + \ln(-1+\sqrt{1+\zeta})\right\}, \end{aligned} \quad (54)$$

where $\zeta = \frac{\pi^2 Q^2}{S^2\beta^2}$. For large β, $M(S,Q)$ reduces to

$$\begin{aligned} M(S,Q) = & -k\frac{b^{-\alpha^2}(4S)^{(\alpha^2+1)/2}}{8\pi(\alpha^2-1)} + \frac{\Lambda(\alpha^2+1)b^{\alpha^2}}{8\pi(\alpha^2-3)}(4S)^{(3-\alpha^2)/2} \\ & + 2\pi Q^2 b^{\alpha^2}(4S)^{(-\alpha^2-1)/2} - \frac{4Q^4\pi^3(\alpha^2+1)b^{\alpha^2}}{\beta^2(\alpha^2+5)}(4S)^{(-\alpha^2-5)/2} + O\left(\frac{1}{\beta^4}\right). \end{aligned} \quad (55)$$

This expression is nothing, but the Smarr-type formula of the topological black holes of EMd theory in the limit $\beta^2 \to \infty$ [14]. Consider S and Q as a complete set of extensive parameters for the mass $M(S,Q)$, one may define the intensive parameters conjugate to S and Q as

$$T = \left(\frac{\partial M}{\partial S}\right)_Q, \qquad U = \left(\frac{\partial M}{\partial Q}\right)_S. \quad (56)$$

It is a matter of calculation to show that the intensive quantities calculated by Eq. (56) coincide with Eqs. (44) and (52). This implies that these quantities satisfy the first law of black hole thermodynamics,

$$dM = TdS + UdQ. \quad (57)$$

IV. THERMAL STABILITY OF THE SOLUTIONS

In this section, we are going to investigate thermal stability of the solutions. The stability of a thermodynamic system with respect to small variations of the thermodynamic coordinates is usually performed by analyzing the behavior of the entropy $S(M,Q)$ around the equilibrium. The energy $M(S,Q)$ can also be the other parameter to study the stability. Depending on the set of thermodynamic variable or state functions of the system, we can study the stability in both canonical and grand canonical ensembles. In the canonical ensemble, the charge is a fixed parameter and therefore the positivity of the heat capacity C_Q is sufficient to ensure the local stability [39,40]. The heat capacity is calculated via

$$C_Q = T\left(\frac{\partial S}{\partial T}\right)_Q = T\left(\frac{\partial^2 M}{\partial S^2}\right)_Q^{-1}. \quad (58)$$

Hence, in the ranges where T is positive, the positivity of $(\partial^2 M/\partial S^2)_Q$ guarantees the local stability of the solutions. Since C_Q has long sentences, so for economic reasons we avoid bringing it here. To have better understanding of the region of stability, we have plotted temperature T and $\partial^2 M/\partial S^2$ in Figs. 24–27. If both T and $\partial^2 M/\partial S^2$ are positive in a special region, so we have stability in that region. It is important to recall that negative temperature is not acceptable physically. For simplicity we have chosen

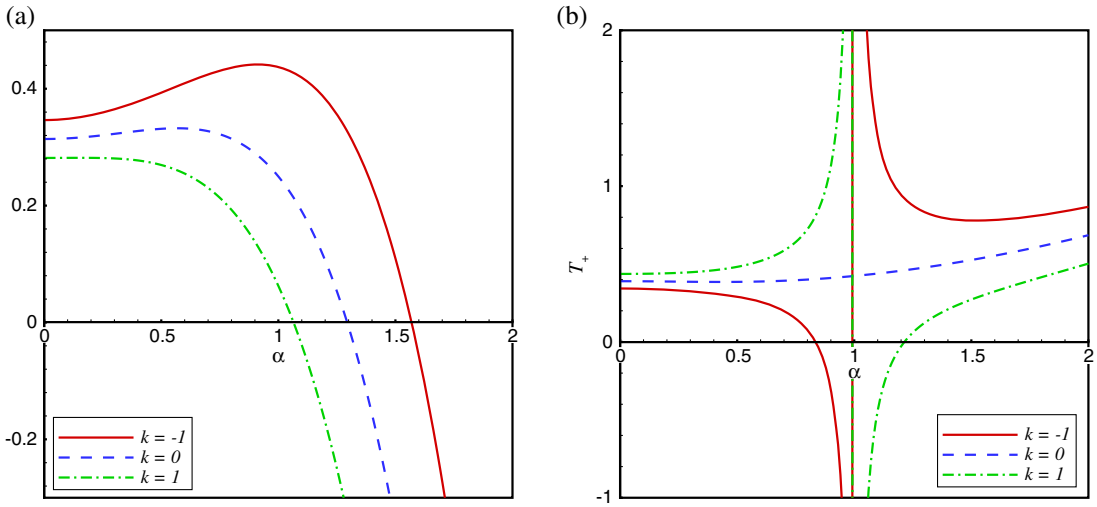

FIG. 24 (color online). Thermal stability for $\beta = 1.5$, $q = 1$, and $r_+ = 1.7$. (a) $\partial^2 M/\partial S^2$ versus α, (b) Temperature versus α.

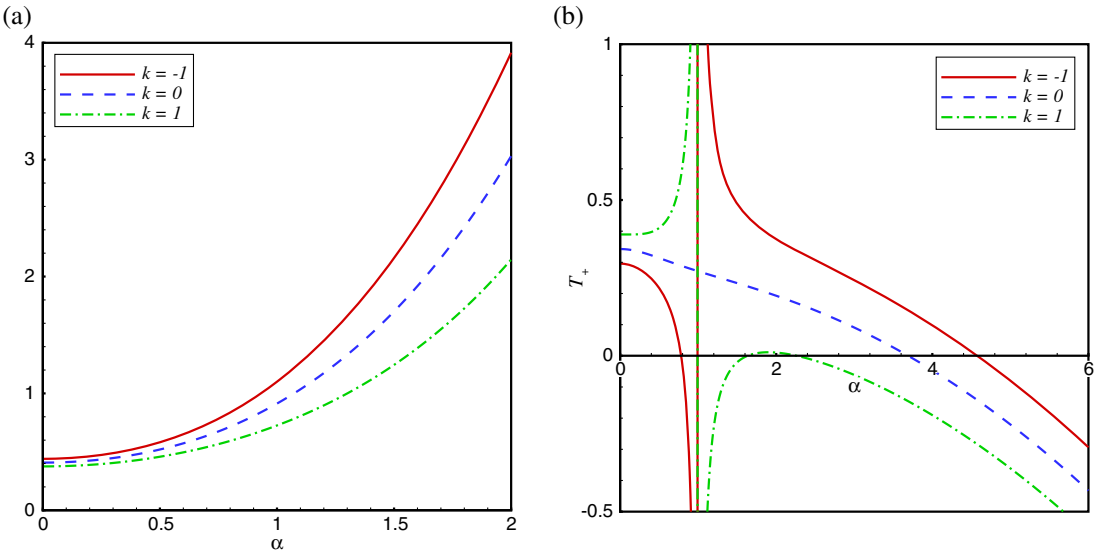

FIG. 25 (color online). Thermal stability for $\beta = 1.5$, $q = 2$, and $r_+ = 1.7$. (a) $\partial^2 M/\partial S^2$ versus α, (b) Temperature versus α.

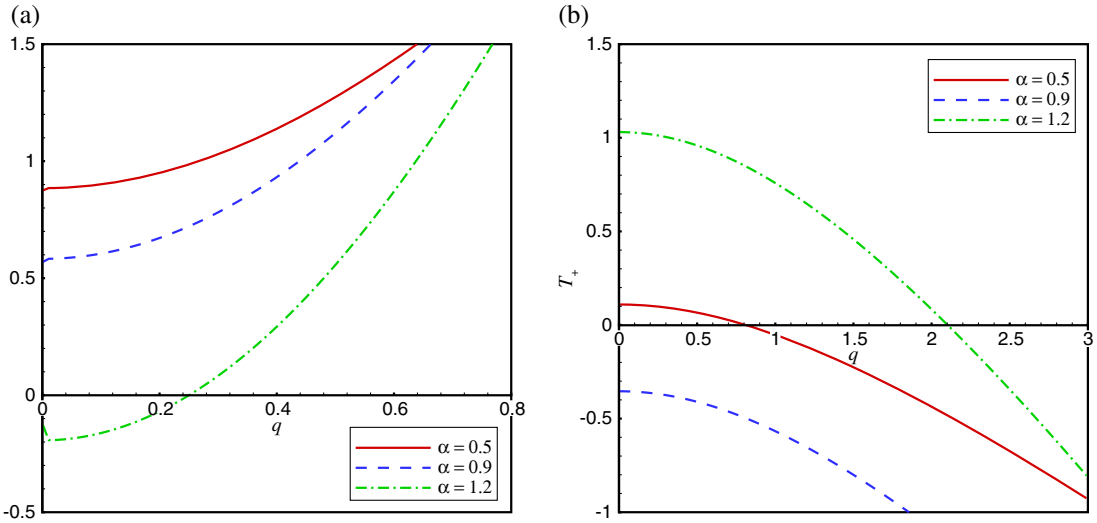

FIG. 26 (color online). Thermal stability for $\beta = 1.5$, $k = -1$, and $r_+ = .8$. (a) $\partial^2 M/\partial S^2$ versus q, (b) Temperature versus q.

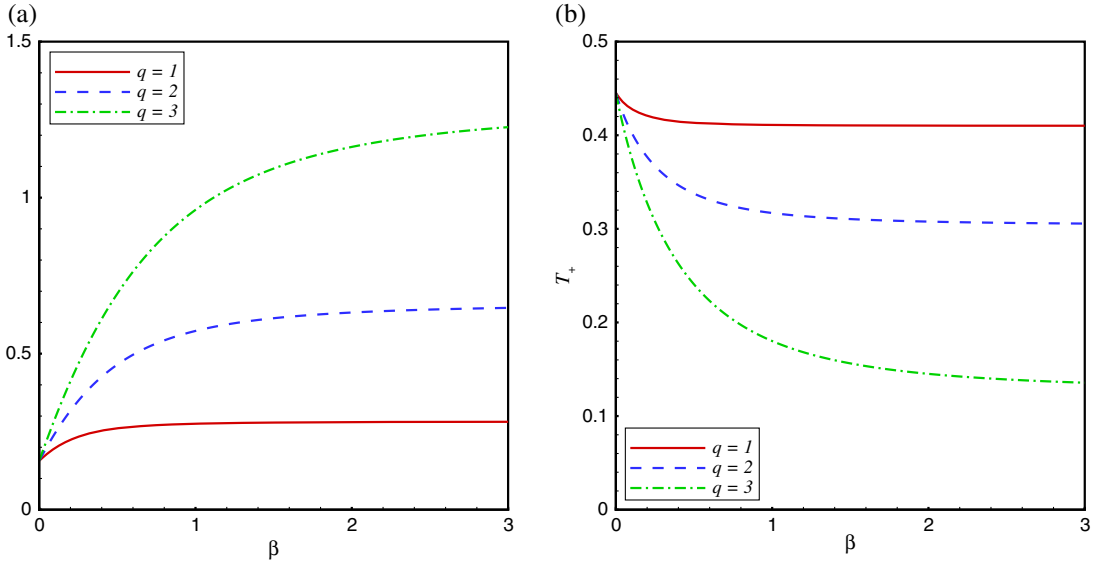

FIG. 27 (color online). Thermal stability for $k = 0$, $\alpha = 0.8$, and $r_+ = 1.8$. (a) $\partial^2 M/\partial S^2$ versus β, (b) Temperature versus β.

$l = b = 1$ in these figures. As one can see from Fig. 24(a), there is a maximum value for the dilaton coupling constant, $\alpha_{\max}$, in which $\partial^2 M/\partial S^2$ is positive for $\alpha < \alpha_{\max}$ and negative for $\alpha > \alpha_{\max}$. The value of $\alpha_{\max}$ depends on the other parameters. On the other hand, $\alpha_{\max}$ decreases with increasing the constant curvature k. By probing the related temperature in 24(b), it is clear that T_+ has a singularity at $\alpha = 1$. T_+ is always positive for $k = 0$. In the case of $k = -1$, T_+ is positive for $\alpha > 1$ but it depends on the value of the other parameters for $\alpha < 1$, while for $k = 1$, T_+ has an inverse behavior. From Fig. 25(a), we see that by increasing q with respect to Fig. 24(a), $\partial^2 M/\partial S^2$ becomes positive for different constant curvature but the temperature tends to have negative value as α gets larger. In Fig. 26(a), we have plotted $\partial^2 M/\partial S^2$ versus q for different α. In this figure for $\alpha < 1$, we see that $\partial^2 M/\partial S^2$ is always positive, but for $\alpha > 1$, the plot comes in the negative region. However, if we investigate the corresponding temperature in Fig. 26(b), we see that $\alpha > 1$ has more action in the positive region. In Fig. 27(a), we have plotted $\partial^2 M/\partial S^2$ versus β for $\alpha < 1$ and different q. For different values of q, $\partial^2 M/\partial S^2$ is positive. It is clear that by increasing q, the value of $\partial^2 M/\partial S^2$ increases too. This implies that increasing q makes the system thermally more stable. Also the corresponding temperature 27(b) is positive for these values of q but by increasing q, the value of $\partial^2 M/\partial S^2$ becomes smaller.

Next, we study stability in the grand canonical ensemble. In the grand canonical ensemble Q is no longer fixed and the positivity of the Hessian matrix guarantees thermal stability of the system. In our case, the mass is a function of entropy and charge and therefore the system is locally stable provided $\mathbf{H}^M_{SQ} > 0$, where the determinant of Hessian matrix can be calculated as

$$\mathbf{H}^M_{SQ} = \begin{bmatrix} H_{11} & H_{12} \\ H_{21} & H_{22} \end{bmatrix}, \tag{59}$$

where

$$H_{11} = \left(\frac{\partial^2 M}{\partial S^2}\right),$$
$$H_{22} = \left(\frac{\partial^2 M}{\partial Q^2}\right),$$
$$H_{12} = H_{21} = \left(\frac{\partial^2 M}{\partial S \partial Q}\right). \tag{60}$$

In this case, entropy and charge are thermodynamic variables. We should consider the region where both Hessian matrix determinant and temperature are positive. We have plotted Figs. 28–31 to investigate stability in the grand canonical ensemble. Again, we have fixed $l = b = 1$. In Fig. 28(a), we showed the behavior of Hessian matrix determinant versus α for different value of β. There is a maximum value for α, called $(\alpha_{\max})$, in which the determinant is positive for $\alpha < \alpha_{\max}$ while it is negative for $\alpha > \alpha_{\max}$. Note that $\alpha_{\max} < 1$ and is independent of the value of nonlinear parameter β. If we investigate the related temperature, the figures are the same. Note that temperature is singular at $\alpha = 1$. For $\alpha < 1$, T_+ is positive while for $\alpha > 1$, its sign depends on the other parameters. In conclusion $\alpha < \alpha_{\max}$ is a reasonable region in which the system is thermally stable. In Fig. 29(a), we have plotted the determinant of the Hessian matrix in terms of q for different value of β. In three curves, we have a $q_{\min}$ for which det(H) is positive for $q > q_{\min}$ but negative for $q < q_{\min}$. The value of $q_{\min}$ is the same for three curves.

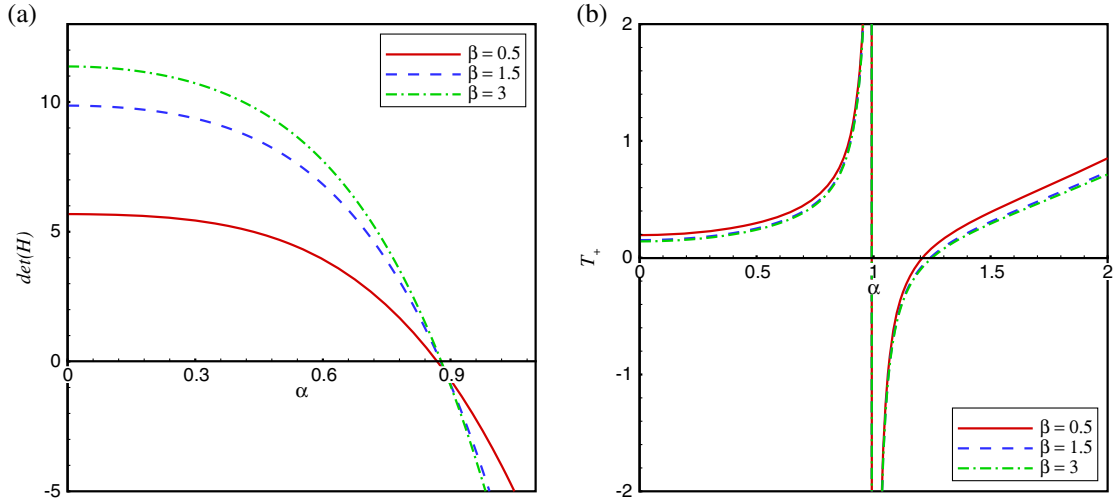

FIG. 28 (color online). Thermal stability in the grand canonical ensemble for $k = 1$, $q = 1$, and $r_+ = 0.8$. (a) $det(H)$ versus α, (b) Temperature versus α.

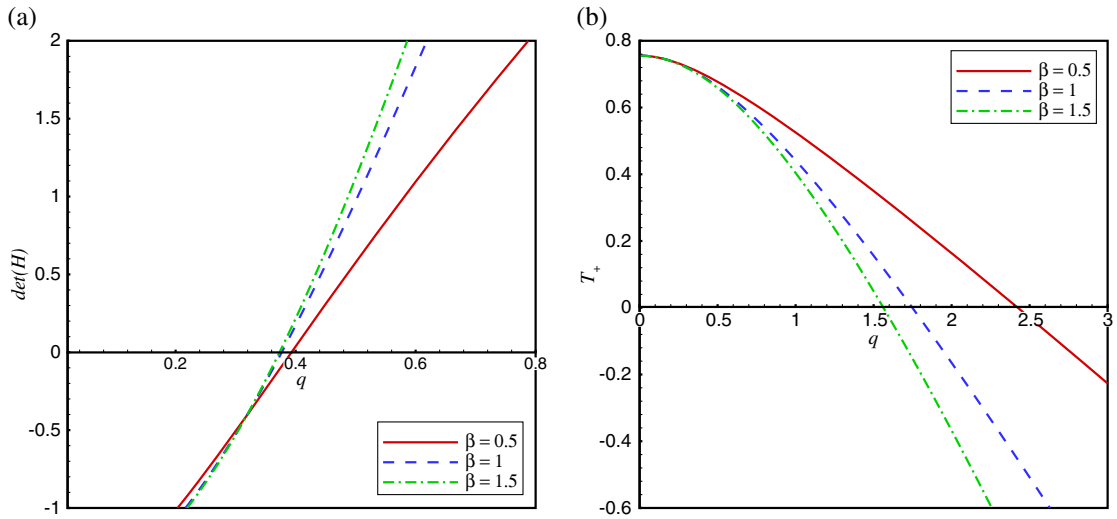

FIG. 29 (color online). Thermal stability in the grand canonical ensemble for $k = 1$, $\alpha = 0.8$, and $r_+ = 0.6$. (a) $det\ (H)$ versus q, (b) Temperature versus q.

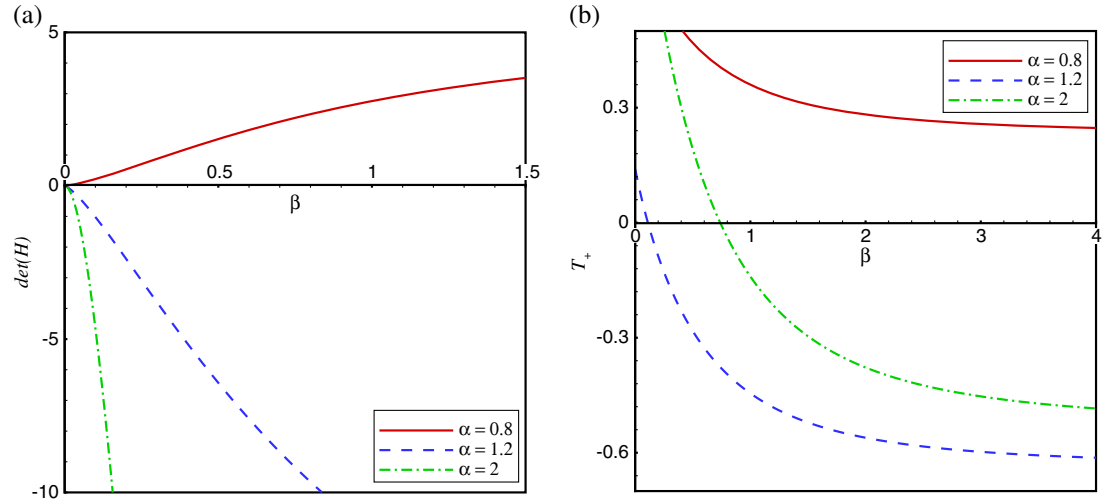

FIG. 30 (color online). Thermal stability in the grand canonical ensemble for $k = 1$, $q = 2$, and $r_+ = 1$. (a) $det(H)$ versus β, (b) Temperature versus β.

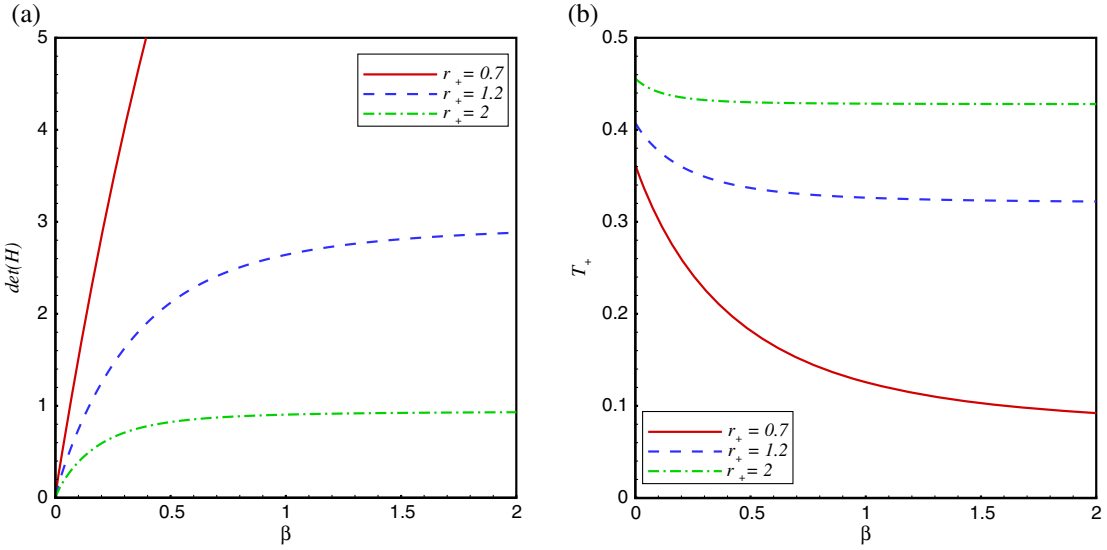

FIG. 31 (color online). Thermal stability in the grand canonical ensemble for $k = 0$, $q = 1$, and $\alpha = 0.8$. (a) $det\ (H)$ versus β, (b) Temperature versus β.

By considering its conjugate temperature, we have a $q_{\max}$, which is different for each curve. Indeed, by decreasing β, the value of $q_{\max}$ increases. For $q < q_{\max}$, the temperature is positive but for $q > q_{\max}$ it is negative. The stable and the physical solutions is in the region that $q_{\min} < q < q_{\max}$. In Fig. 30(a) we see that for $\alpha < 1$, both determinant of the Hessian matrix and temperature are positive, while for $\alpha > 1$, the determinant of the Hessian matrix is negative, so we cannot have stability for these cases. Finally, in Fig. 31(a), we have plotted Hessian matrix determinant versus β for different r_+. By increasing r_+, the value of det(H) goes to 0 but all of them are in the positive region. Also, temperature increases by increasing r_+. So for these ranges of the parameters, our solutions are thermally stable.

V. GEOMETROTHERMODYNAMICS

In the final section we would like to investigate phase transition by using the method of geometry in thermodynamics (GTD). GTD is a method that describes the properties of thermodynamic systems in terms of concepts of differential geometry. This method was first developed by Weinhold [41] who introduced in the equilibrium space a Riemannian metric defined in terms of the second derivatives of the internal energy with respect to entropy and other extensive variables of a thermodynamic system. Then, Ruppeiner [42] proposed a Riemannian metric structure in thermodynamic fluctuation theory, and related it to the second derivatives of the entropy. The Ruppeiner metric is based on the thermodynamic state space geometry.

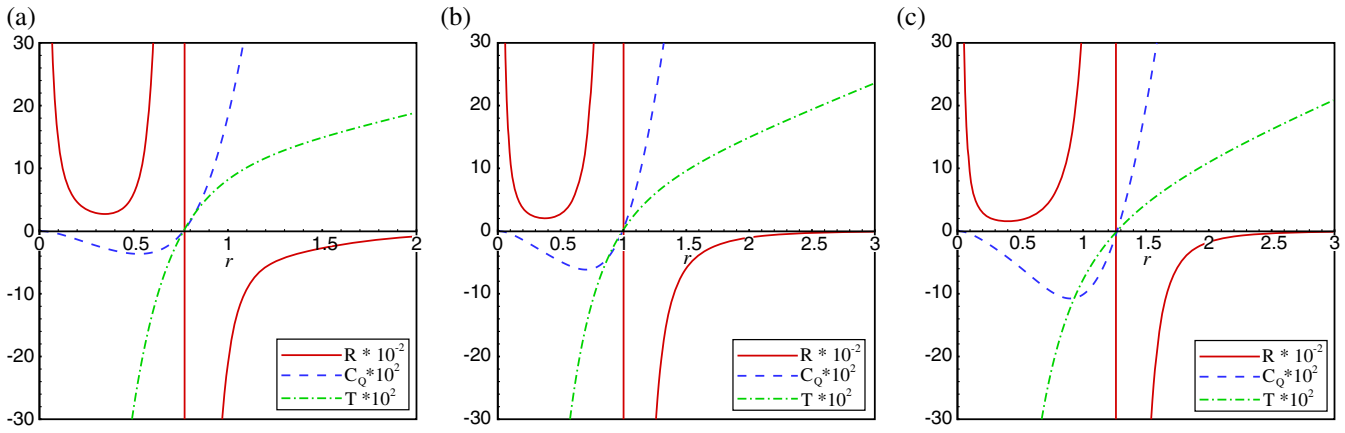

FIG. 32 (color online). Ricci scalar (R), heat capacity (C_Q), and temperature(T) versus r_+ for $\alpha = 0$ and $\beta = 2$. (a) $k = 1$, (b) $k = 0$, (c) $k = -1$.

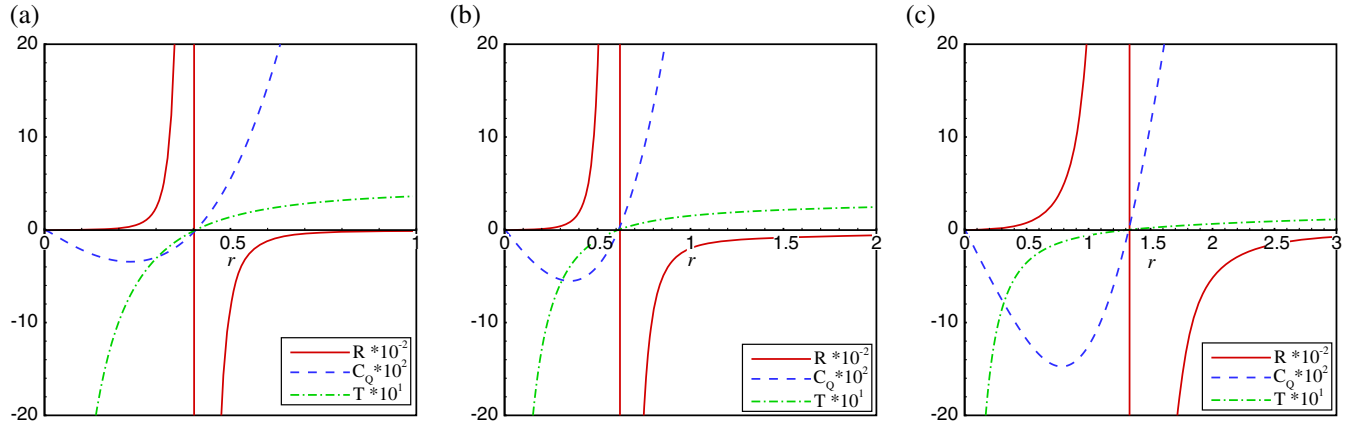

FIG. 33 (color online). Ricci scalar (R), heat capacity (C_Q), and temperature(T) versus r_+ for $\alpha = 0.8$ and $\beta = 1$. (a) $k = 1$, (b) $k = 0$, (c) $k = -1$.

For the second order phase transitions, the Ruppeiner scalar curvature, R, is expected to diverge at the critical points. We should note that Ruppeiner's metric is conformally related to the Weinhold's metric with the inverse temperature as the conformal factor [43]. Sometimes, the singular points of the Weinhold and Ruppeiner metrics do not coincide with the ones of the heat capacity, unfortunately that causes us to go to other methods. Then Quvedo proposed another geometric formulation of thermodynamics [44–47] to solve this problem. Quvedo's metric was invariant under Legendre transformation. Now we introduce a new Legendre invariant metric,

$$ds^2 = -S\frac{\partial}{\partial S}M(S,Q)\frac{\partial^2}{\partial S^2}M(S,Q)dS^2 + S\frac{\partial}{\partial S}M(S,Q)\frac{\partial^2}{\partial Q^2}M(S,Q)dQ^2. \quad (61)$$

Based on metric (61), we calculate the Ricci scalar, R. Since R has long sentences and for the economic reason, we avoid bringing it here. However, we plot the behavior of R for different values of the parameters in Figs. 32–34. In addition to the Ricci scalar, we have also plotted the behavior of heat capacity (58) and temperature to investigate phase transition points. In these figures, we have fixed $b = 2$ and $l = 1$, for simplicity. As one can see, these figures have different behavior for $\alpha < 1$ and $\alpha > 1$. For $\alpha < 1$, the Ricci scalar diverges exactly at the point where both T and C_Q become zero. At this point we have a phase transition. This kind of phase transition happens when the black hole changes its behavior from an unreal case to a real case because C_Q goes from the negative region to the positive region. For $\alpha > 1$, in addition to the first point where T and C_Q are zero and the Ricci scalar becomes infinite, we have an additional point for which T is positive and both C_Q and the Ricci scalar diverge. In this second point we have a first order phase transition. This kind of phase transition happens when the black hole changes from a larger size to a smaller one or vice versa. The effects of the curvature constant k is only a shifting in these points as one can see from the figures. Indeed, with decreasing k the point of divergency increases.

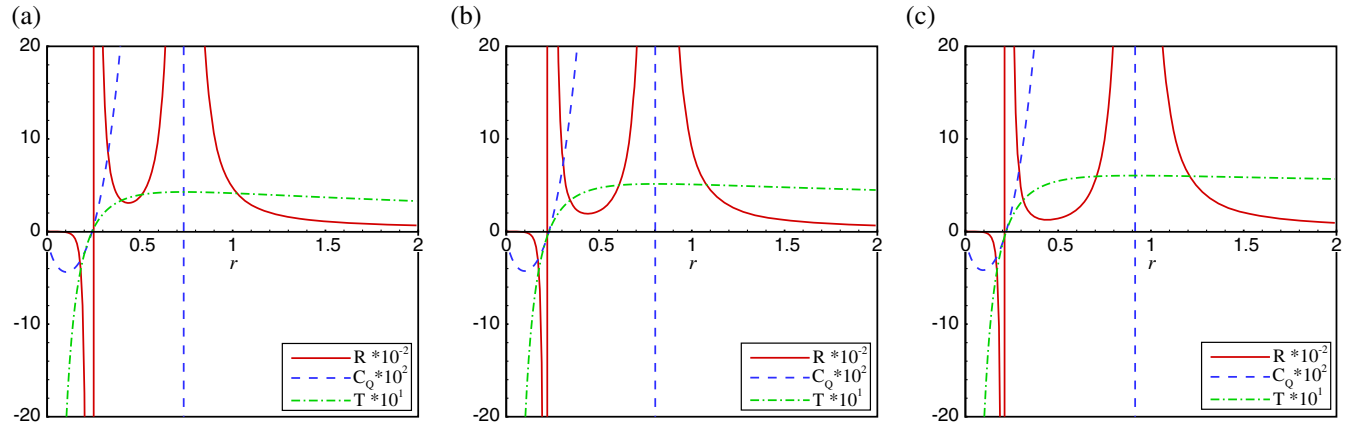

FIG. 34 (color online). Ricci scalar(R), heat capacity (C_Q), and temperature(T) versus r_+ for $\alpha = \sqrt{2}$ and $\beta = 1$. (a) $k = 1$, (b) $k = 0$, (c) $k = -1$.

VI. CONCLUSION AND DISCUSSION

In this paper, we generalized the study on the logarithmic nonlinear electrodynamics to dilaton gravity. For this purpose, we considered an action in which gravity is coupled to dilaton and logarithmic nonlinear electrodynamics. As far as we know, this is for the first time that Lagrangian (6) is introduced in the literature. Then, by varying the action we obtained the field equations. By choosing the potential associated with the dilaton field in the form of Liouville-type with two terms, as given in (5), we constructed a new class of topological black hole solutions of this theory. We found that these solutions can describe black holes with two horizons, an extreme black holes or a naked singularity depending on the model parameters. In the case of $k = \pm 1$ our solutions do not exist for the string case where $\alpha = 1$. Besides for $\alpha \neq \sqrt{3}$, our solutions are ill-defined. We found that, in contrast to the linear Maxwell theory, the electric field can have finite value *near the origin* where $r \to 0$. Indeed, we found out that the divergency of the electric field *near the origin*, increases with increasing the dilaton coupling parameter α. Besides, the divergency of the electric field *near the origin* for LNd is weaker than EMd and stronger than BId theory. We also showed that near the origin and for fixed r, with increasing α, the electric field of BId and LNd black holes approaches to the electric field of EMd black holes.

In order to study the casual structure of the spacetime, we investigated the behavior of the metric function $f(r)$ versus r for different model parameters. Interestingly enough, we found that in the case of $k = 1$ and fixed value of m, α, and q, there is a minimum (extreme) value for the nonlinear parameter $\beta_{\rm min}(\beta_{\rm ext})$, for which we have a black hole with a nonextreme horizon provided $\beta \leq \beta_{\rm min}$, black hole with two horizons for $\beta_{\rm min} < \beta < \beta_{\rm ext}$, black hole with an extreme horizon for $\beta = \beta_{\rm ext}$ and naked singularity for $\beta > \beta_{\rm ext}$. When $\alpha = \gamma = 0$ our solutions reduce to the four-dimensional topological black hole solutions of LN electrodynamics [31], while in the limit $\beta \to \infty$ they reduce to the topological black holes of EMd gravity [14].

We also computed the charge, mass, temperature, entropy, and electric potential of the topological dilaton black holes and verified that these quantities satisfy the first law of black hole thermodynamics. The satisfaction of the first law of thermodynamics for the obtained conserved and thermodynamic quantities, together with the fact that these quantities in two limiting cases, namely in the absence of the dilaton field ($\alpha = 0 = \gamma$), and for large values of the nonlinear parameter ($\beta \to \infty$), reduce to the known results of LN theory [31] and EMd gravity [14], respectively, indicate that the conserved and thermodynamic quantities obtained in this paper are correct and in agreement with other methods such as the Euclidean action method [48]. Then, we investigated thermal stability of the solutions in canonical and grand canonical ensembles. For stability in the canonical ensemble, the heat capacity should be positive. For example for $k = 0$ and different value of q, we have thermally stable solution for an arbitrary β. In grand canonical ensemble, both the Hessian matrix determinant and temperature should be positive. For example, for $k = 1$, if $\alpha < 1$, the solutions are thermally stable, while for $\alpha > 1$, the system is in an unstable phase. At the end we found phase transition points using the method of thermodynamical geometry of the solutions. For this purpose, we proposed a new metric and calculated the related Ricci scalar. This metric was a good choice because the phase transition occurs at the point that the Ricci scalar becomes either zero or infinity. For $\alpha < 1$, we have a type of phase transition that the Ricci scalar becomes zero, while for $\alpha > 1$, in addition to the first point we have a first order phase transition in which the Ricci scalar becomes infinity.

Although, in this paper we constructed static topological dilaton black holes in the presence of logarithmic nonlinear electrodynamics, many issues however still remain to be investigated. For example, it would be nice to derive rotating black hole/string solutions of these field equations. It is also interesting to generalize the study to higher dimensions and construct both static and rotating black holes/branes of LNd theory in arbitrary dimensions. Magnetic rotating string/brane solutions of this theory is another subject which can be explored. These issues are now under investigation and the results will appear soon.

ACKNOWLEDGMENTS

We thank referees for constructive comments which helped us improve the paper significantly. We thank Shiraz University Research Council. The work of A. Sheykhi has been supported financially by Research Institute for Astronomy and Astrophysics of Maragha, Iran.

[1] M. B. Green, J. H. Schwarz, and E. Witten, *Superstring Theory* (Cambridge University Press, Cambridge, England, 1987).

[2] S. Mignemi and D. Wiltshire, Classical Quantum Gravity **6**, 987 (1989); D. L. Wiltshire, Phys. Rev. D **44**, 1100 (1991); S. Mignemi and D. L. Wiltshire, Phys. Rev. D **46**, 1475 (1992).

[3] S. J. Poletti and D. L. Wiltshire, Phys. Rev. D **50**, 7260 (1994).

[4] K. C. K. Chan, J. H. Horne, and R. B. Mann, Nucl. Phys. **B447**, 441 (1995).

[5] R. G. Cai, J. Y. Ji, and K. S. Soh, Phys. Rev. D **57**, 6547 (1998); R. G. Cai and Y. Z. Zhang, Phys. Rev. D **64**, 104015 (2001).

[6] G. Clement, D. Gal'tsov, and C. Leygnac, Phys. Rev. D **67**, 024012 (2003); G. Clement and C. Leygnac, Phys. Rev. D **70**, 084018 (2004).

[7] T. Ghosh and P. Mitra, Classical Quantum Gravity **20**, 1403 (2003).

[8] M. H Dehghani and N. Farhangkhah, Phys. Rev. D **71**, 044008 (2005).

[9] A. Sheykhi, M. H. Dehghani, and N. Riazi, Phys. Rev. D **75**, 044020 (2007).

[10] A. Sheykhi, M. H. Dehghani, N. Riazi, and J. Pakravan, Phys. Rev. D **74**, 084016 (2006).

[11] S. S. Yazadjiev, Phys. Rev. D **72**, 044006 (2005).

[12] S. S. Yazadjiev, Classical Quantum Gravity **22**, 3875 (2005).

[13] A. Sheykhi, N. Riazi, and M. H. Mahzoon, Phys. Rev. D **74**, 044025 (2006).

[14] A. Sheykhi, Phys. Rev. D **76**, 124025 (2007).

[15] M. Born and L. Infeld, Proc. R. Soc. A **144**, 425 (1934).

[16] E. Fradkin and A. Tseytlin, Phys. Lett. **163B**, 123 (1985); R. Matsaev, M. Rahmanov, and A. Tseytlin, Phys. Lett. B **193**, 207 (1987); E. Bergshoeff, E. Sezgin, C. Pope, and P. Townsend, Phys. Lett. B **188**, 70 (1987).

[17] C. Callan, C. Lovelace, C. Nappi, and S. Yost, Nucl. Phys. **B308**, 221 (1988); O. Andreev and A. Tseytlin, Nucl. Phys. **B311**, 205 (1988); R. Leigh, Mod. Phys. Lett. A **04**, 2767 (1989).

[18] H. H. Soleng, Phys. Rev. D **52**, 6178 (1995).

[19] S. H. Hendi, J. High Energy Phys. 03 (2012) 065; S. H. Hendi and A. Sheykhi, Phys. Rev. D **88**, 044044 (2013).

[20] A. Sheykhi and S. Hajkhalili, Phys. Rev. D **89**, 104019 (2014).

[21] A. Sheykhi and A. Kazemi, Phys. Rev. D **90**, 044028 (2014).

[22] M. Kord Zangeneh, A. Sheykhi, and M. H. Dehghani, Phys. Rev. D **91**, 044035 (2015).

[23] A. Sheykhi and N. Riazi, Phys. Rev. D **75**, 024021 (2007); A. Sheykhi, Int. J. Mod. Phys. D **18**, 25 (2009).

[24] A. Sheykhi, Phys. Lett. B **662**, 7 (2008).

[25] T. Tamaki and T. Torii, Phys. Rev. D **62**, 061501R (2000).

[26] T. Tamaki and T. Torii, Phys. Rev. D **64**, 024027 (2001).

[27] R. Yamazaki and D. Ida, Phys. Rev. D **64**, 024009 (2001).

[28] G. Clement and D. Gal'tsov, Phys. Rev. D **62**, 124013 (2000).

[29] S. S. Yazadjiev, P. P. Fiziev, T. L. Boyadjiev, and M. D. Todorov, Mod. Phys. Lett. A **16**, 2143 (2001).

[30] M. H Dehghani, S. H. Hendi, A. Sheykhi, and H. Rastegar Sedehi, J. Cosmol. Astropart. Phys. 02 (2007) 020; M. H. Dehghani, A. Sheykhi, and S. H. Hendi, Phys. Lett. B **659**, 476 (2008).

[31] S. H. Hendi, Ann. Phys. (N.Y.) **333**, 282 (2013).

[32] D. R. Brill, J. Louko, and P. Peldan, Phys. Rev. D **56**, 3600 (1997).

[33] R. G. Cai and K. S. Soh, Phys. Rev. D **59**, 044013 (1999).

[34] R. B. Mann, Classical Quantum Gravity **14**, 2927 (1997).

[35] J. Maldacena, Adv. Theor. Math. Phys. **2**, 231 (1998); E. Witten, Adv. Theor. Math. Phys. **2**, 253 (1998); O. Aharony, S. S. Gubser, J. Maldacena, H. Ooguri, and Y. Oz, Phys. Rep. **323**,183 (2000); V. Balasubramanian and P. Kraus, Commun. Math. Phys. **208**, 413 (1999).

[36] S. de Haro, K. Skenderis, and S. N. Solodukhin, Commun. Math. Phys. **217**, 595 (2001).

[37] J. Brown and J. York, Phys. Rev. D **47**, 1407 (1993); J. D. Brown, J. Creighton, and R. B. Mann, Phys. Rev. D **50**, 6394 (1994).

[38] S. H. Hendi, A. Sheykhi, and M. H. Dehghani, Eur. Phys. J. C **70**, 703 (2010).

[39] A. Chamblin, R. Emparan, C. V. Johnson, and R. C. Myers, Phys. Rev. D **60**, 104026 (1999).

[40] P. C. W. Davies, Proc. R. Soc. A **353**, 499 (1977).

[41] F. Weinhold, J. Chem. Phys. **63**, 2479 (1975).

[42] G. Ruppeiner, Phys. Rev. A **20**, 1608 (1979).

[43] P. Salamon, J. D. Nulton, and E. Ihrig, J. Chem. Phys. **80**, 436 (1984).

[44] H. Quevedo, J. Math. Phys. (N.Y.) **48**, 013506 (2007).

[45] H. Quevedo, Gen. Relativ. Gravit. **40**, 971 (2008).

[46] H. Quevedo, A. Sanchez, S. Taj, and A. Vazquez, Gen. Relativ. Gravit. **43**, 1153 (2011).

[47] H. Quevedo, Gen. Relativ. Gravit. **40**, 971 (2008).

[48] O. Miskovic and R. Olea, Phys. Rev. D **77**, 124048 (2008).